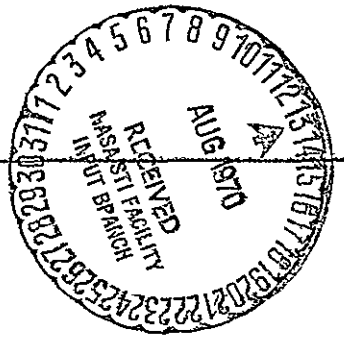

BIAXIAL STRENGTH OF MIG- AND TIG-WELDED 2014-T6 AT 70°, -320° AND -423°F

DAC 62102

GLAS
MISSILE & SPACE SYSTEMS DIVISION

BIAXIAL STRENGTH OF MIG- AND TIG-WELDED 2014-T6 AT 70°, -320° AND -423°F

DOUGLAS REPORT DAC 62102
DATE· 5-24-68

Prepared by R. A. Rawe
Metallurgical Development
Metallurgy Branch, MR&PM

Prepared for

National Aeronautics and
Space Administration
Marshall Space Flight Center
Huntsville, Alabama
Contract NAS7-101

Approved by G. V. Bennett
Branch Chief, Metallurgy, MR&PM
Santa Monica Development Engineering

Catalog No. PDL 86784

ACKNOWLEDGEMENT

This report summarizes work performed by a number of individuals and groups within MSSD D A Eitman was responsible for directing fabrication of the biaxial specimens The SATURN Structural Test Section was responsible for designing of a special biaxial testing machine, performing the biaxial tests and reducing the test data D L Corn and J Green conducted failure analyses of the biaxial specimens after testing

ABSTRACT

A test program was conducted to develop biaxial strength allowables for MIG and TIG welds in 2014-T6 aluminum Welded cylinders, 16-in in diameter and 60-in. long, were fabricated using procedures simulating actual production methods used for SATURN S-IVB domes and common bulkheads Certain of the specimens were subjected to a thermal curing cycle The cylinders, each having two diametrically opposite longitudinal welds, were tested to failure at 70°, -320° and -423°F by combined internal pressurization and applied axial loading producing biaxial stress states of either 2-to-1 (axial-to-hoop) or 1-to-1 (axial-to-hoop) Under all test conditions the TIG-welded specimens exhibited greater biaxial strength than the MIG-welded specimens

TABLE OF CONTENTS

LIST OF FIGURES

LIST OF FIGURES (Cont'd)

LIST OF TABLES

INTRODUCTION

The purpose of this program was the development of biaxial strength allowables as related to MIG and TIG welding of SATURN S-IVB domes and common bulkheads It consisted of fabricating and testing twenty-one MIG welded and twenty-one TIG welded 2014-T6 16-inch diameter cylinders Besides the welding process, test variables included test temperature, biaxial stress state, and number of cures (uncured and double-cured)

The test cylinders were fabricated to simulate actual production fabrication methods. The welding procedures (MIG) simulated those employed in meridional welds of the S-IVB common bulkhead

The common bulkhead is a double-walled, spherical-contour membrane separating the liquid hydrogen and liquid oxygen tanks of the S-IVB vehicle Insulation, which is cured in place, is provided between the forward (LH_2 side) and aft (LOX side) domes of the bulkhead During operation the forward dome is in contact with liquid hydrogen ($-423^{\circ}F$) and the aft dome is in contact with liquid oxygen ($-298^{\circ}F$) The aft dome of the S-IVB encloses the liquid oxygen tank and during operation is in contact with liquid oxygen at $-298^{\circ}F$ The entire tank assembly is proof tested at $70^{\circ}F$ The test temperatures for the program, $70^{\circ}F$, $-320^{\circ}F$ and $-423^{\circ}F$, were selected to simulate operating and proof temperatures of the tank assembly

Figure 1 illustrates some of the stress states which can be experienced in a cylindrical pressure vessel with hemispherical domes The stress state in the weld joints can depend upon the thickness of the weld relative to the thickness of the membrane In a uniform-thickness, hemispherical

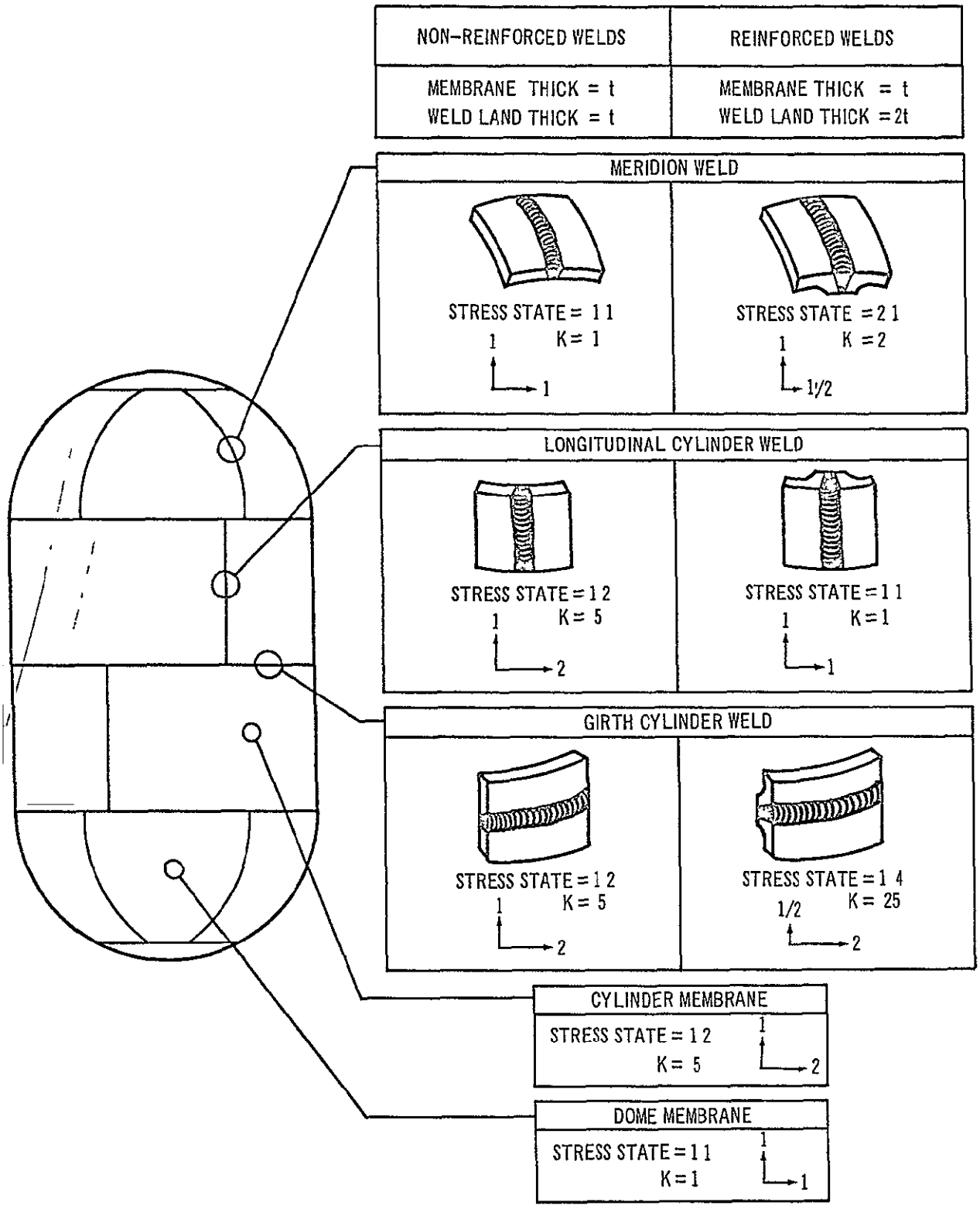

Figure 1 Biaxial Stress States in a Pressure Vessel

$$K = \frac{\text{Axial Stress}}{\text{Hoop Stress}}$$

dome the stress state due to internal pressure is 1-to-1 (axial-to-hoop) Weld land reinforcement in meridian welds, used when the strength of the weld is less than the strength of the parent metal, can reduce the stress (hoop) normal to the weld The stress parallel with the weld (axial) is not reduced by weld land reinforcement provided that the strain in the weld land tends to equal the strain in the membrane If the weld thickness is exactly twice the membrane thickness, the stress state in the meridian weld is 2-to-1 (axial-to-hoop) while the dome membrane stress state remains 1-to-1 The biaxial stress states employed in the test program were 1-to-1 and 2-to-1 (axial-to-hoop)

PROCEDURE

The biaxial test matrix is shown in Table 1 Tests of cured specimens represent the common bulkhead which experiences temperatures in the range 70° to $-423^{\circ}F$ Tests of uncured specimens represent the aft (LOX) dome which experiences temperatures in the range 70° to $-298^{\circ}F$

Material and Specimen Preparation

The raw material for this work was selected from stock originally purchased for the SATURN S-IVB program The original thickness of the 2014 sheet stock was 0 143 in Type 4043 weld filler wire was used, MIG welds were made using 0 045 in diameter wire and TIG welds were made with 0 062-in diameter wire

The biaxial test specimens were 16-in diameter cylinders 60-in in length, as shown in Figure 2

TABLE 1

BIAXIAL TEST MATRIX

Cure Cycles	Stress State (Axial-to-Hoop)	Test Temperature °F	MIG Welded Specimens	TIG Welded Specimens
None	1-to-1	70°	3	3
		-320°	3	3
	2-to-1	70°	3	3
		-320°	3	3
Cure Cycles of Common B/H No 2002	2-to-1	70°	3	3
		-320°	3	3
		-423°	3	3

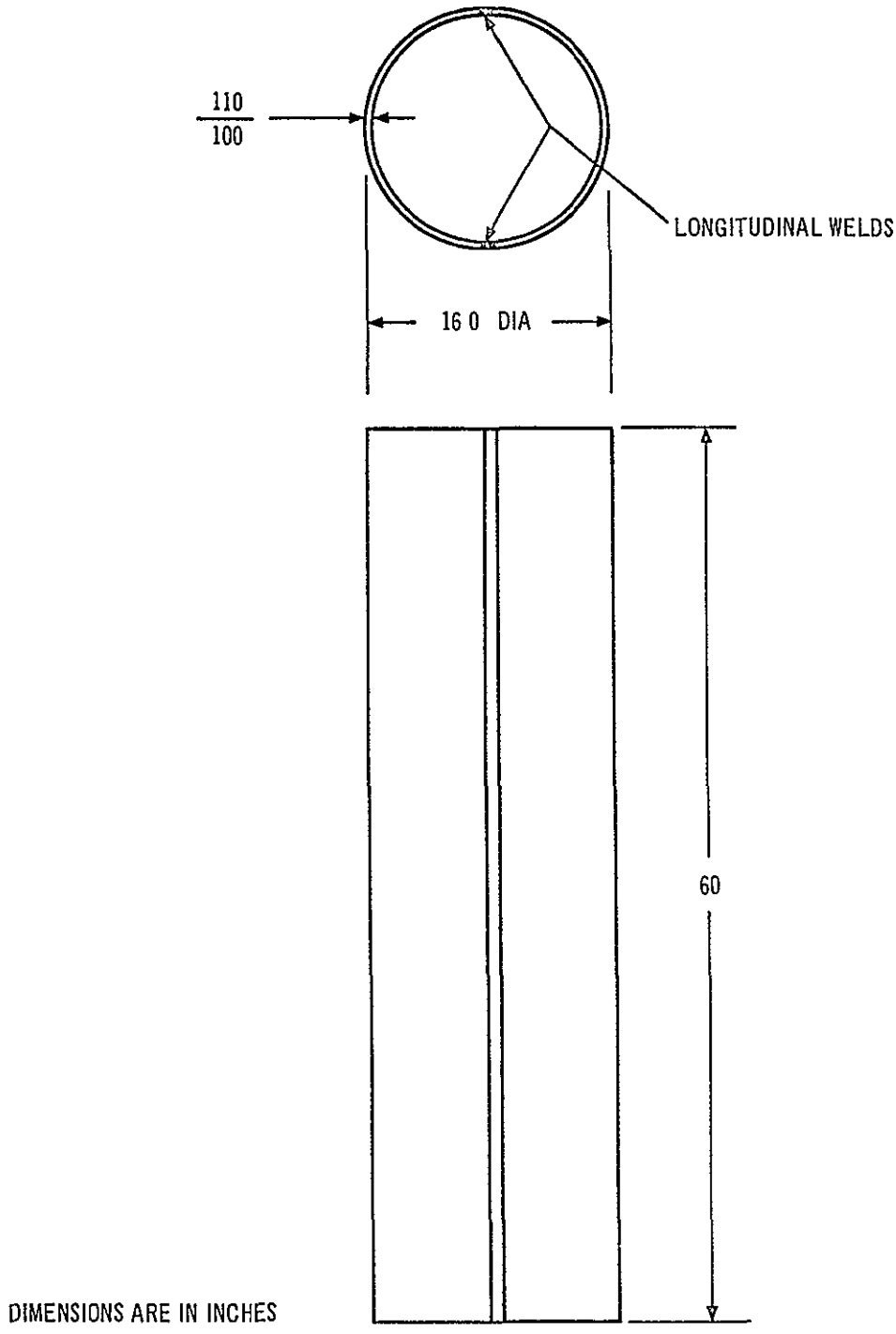

Figure 2 Welded Biaxial Test Cylinder Dimensions

The manufacturing flow chart for the biaxial specimens is shown in Figure 3. The cylindrical specimens were assembled by the joining of two semi-cylinders formed from sheet. Blanks, approximately 73-in long by 25-in wide, were sheared and chem-milled to a final thickness of 0 105-in (thickness tolerances of ± 0 005-in). After chem-milling, the blanks were annealed according to DPS 7 00-1, as shown in Table 2 Annealed blanks were formed to a semi-cylindrical shape (8-in radius) on a stretch brake and solution treated according to DPS 7 00-1 (Table 2) Prior to aging to the -T6 condition, the semi-cylinders were sized on the stretch brake All aged semi-cylinders were anodized and trimmed to size for welding

Before welding, the joints were cleaned according to DPS 9 14 A nitric-hydrofluoric acid slurry (Pasa-Jel) was used to loosen the anodized coating from the joint surfaces The slurry was removed by use of British Etch Just prior to welding, the joint edges were hand filed All welds were made using 4043 filler wire by either the MIG or the TIG process Weld parameters are listed in Table 3

After welding, the welds were shaved to within 0 010-in. of the parent metal thickness on both the inside and outside surfaces of the cylinders All welds were radiographed and inspected with dye penetrant Those cylinders scheduled to be tested in the "cured" condition were then subjected to cure cycles simulating those actually used on S-IVB Common Bulkhead SN 2002 (P/N 1A 39309).

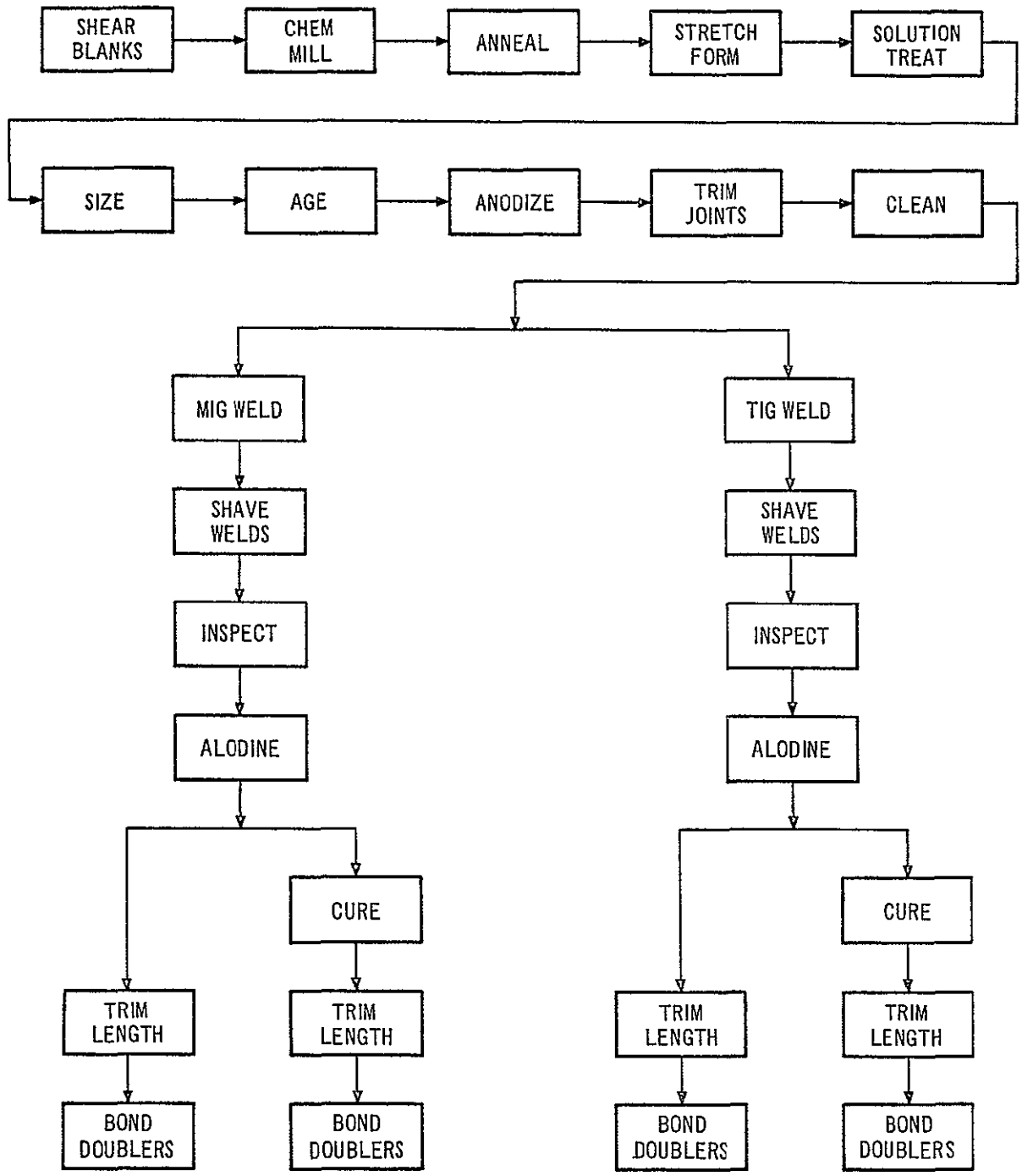

Figure 3 Manufacturing Flow Chart for Production of Biaxial Test Specimens

TABLE 2

HEAT TRFATMENTS USED FOR PROCESSING 2014 (1)

Anneal	Solution Treat	Age - T6
1 1-hour heating time	1 40-55 minutes in air at 925-945°F	1 19-hours in air at 310-330°F
2 2-hour soak at 780°F	2 Water quench	2 Air cool to room temperature
3. Furnace cool to 500°F (not faster than 50°F/hr)		
4 Air cool to room temperature		

(1) DPS 7 00-1

TABLE 3

WELDING PARAMETERS USED IN FABRICATION OF TEST SPECIMENS

PARAMETER	MIG	TIG
Weld Unit	Linde SVI 500 #1554 with Linde Travel Governor Control	Miller 360 A/BP with Linde SVI 500 Wire Feed
Finger Pressure	100 psi (8 ft Airline Fixture)	100 psi (8 ft Airline Fixture)
Chill Bar	Titanium with 0 312 in by 0 040 in slot	Copper with 0 260 in by 0 025 in slot
Torch	Linde ST5 with #8 Cup	Linde HW 27 with #10 Cup
Lead Angle	10°	10°
Contact Tube	0 057 in	- - - -
Slope	Flat with Dial at 8	- - - -
Voltage Range of Slope	13-34	- - - -
Inductor	Low-Dial at 4	- - - -
Atmosphere	Pure Argon	Pure Helium
Flow Rate	60 cu ft /hr	70-100 cu ft /hr
Weld Wire	Type 4043, Wire Spool, 0 045 in dia , Heat #044U	Type 4043, 0 063 in dia
Current	135-138 amps	138-147 amps
Voltage	22-25 Volts	11-1/2 - 12-1/4 Volts
Travel Rate	28 in /min	15 in /min.
Electrode	- - - -	3/32 in dia Tungsten 2% Thoria
Wire Feed	- - - -	38-52 in /min

Cylinders were cut to length and the trim was used for uniaxial tensile specimens. Doublers, as shown in Figure 4, were bolted and adhesively bonded to the cylinder ends using Narmco 7343 This adhesive requires a cure cycle of 160°F for 24 hours The doublers provided attachment sites for the loading heads which also seal the cylinder The doublers were designed with fingers to minimize end effects

Each aluminum loading head contained a 16-in diam circular groove into which the test cylinder was inserted for attachment Molten Cerrobend alloy (melting point 159°F) filled the groove and solidified locking the cylinder in place After solidification the Cerrobend alloy undergoes a solid state reaction which results in a volume expansion Such expansion within the circular groove established a gas-tight seal between the cylinder and the loading head Loading heads for room temperature tests are shown schematically in Figure 5 Cryogenic loading heads, shown in Figure 6, were designed to trap the helium gas used for pressurization and to release slowly the expanding gas at failure to produce a hydrostatic, rather than a pneumatic, burst In addition, the baffle arrangement kept the warm helium gas from contacting the specimen walls

Test Equipment

As detailed in Reference (1), some room temperature biaxial tests were performed in a Baldwin 400,000 lb capacity testing machine with an auxiliary hydraulic pressurization system The Baldwin testing machine was used to apply axial loads and the hydraulic system was used to

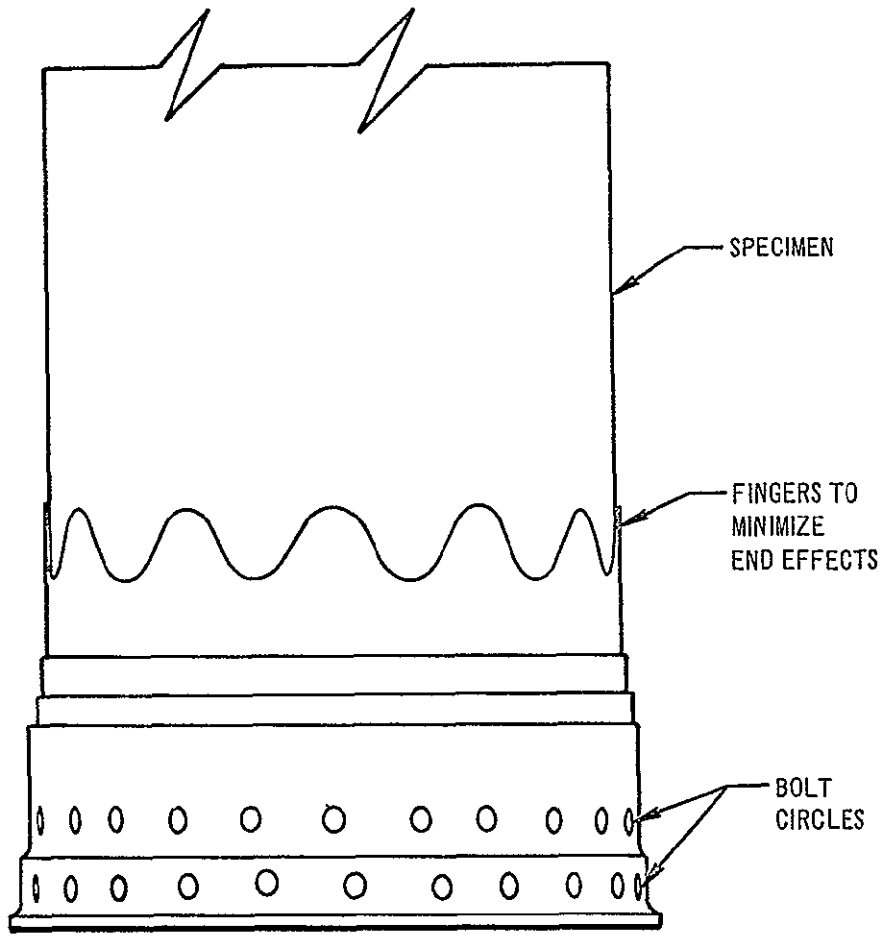

Figure 4 Bonded and Bolted End–Doubler Attached to Each End of Biaxial Test Cylinder

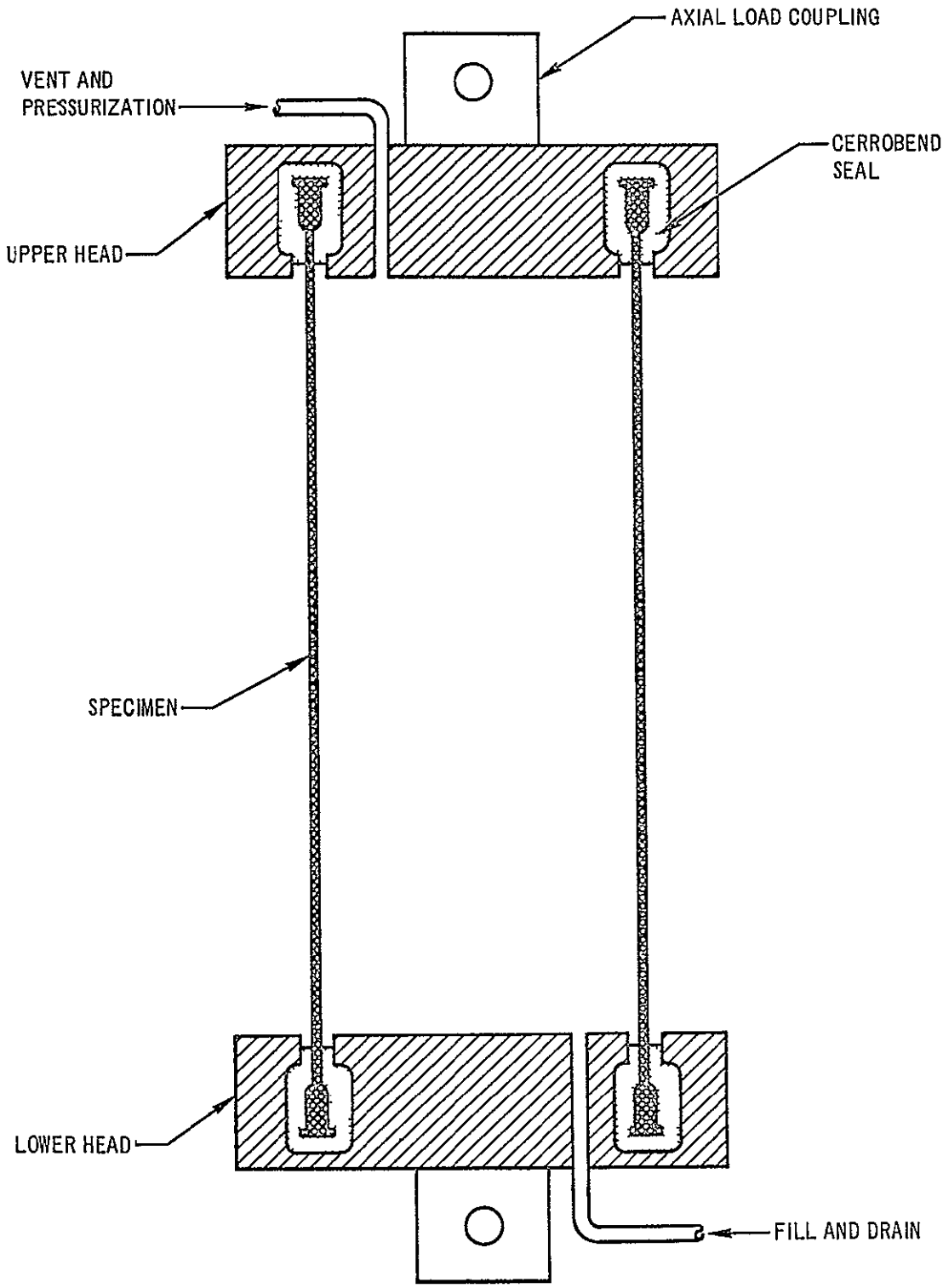

Figure 5 Biaxial Specimen Assembly for Room Temperature Tests

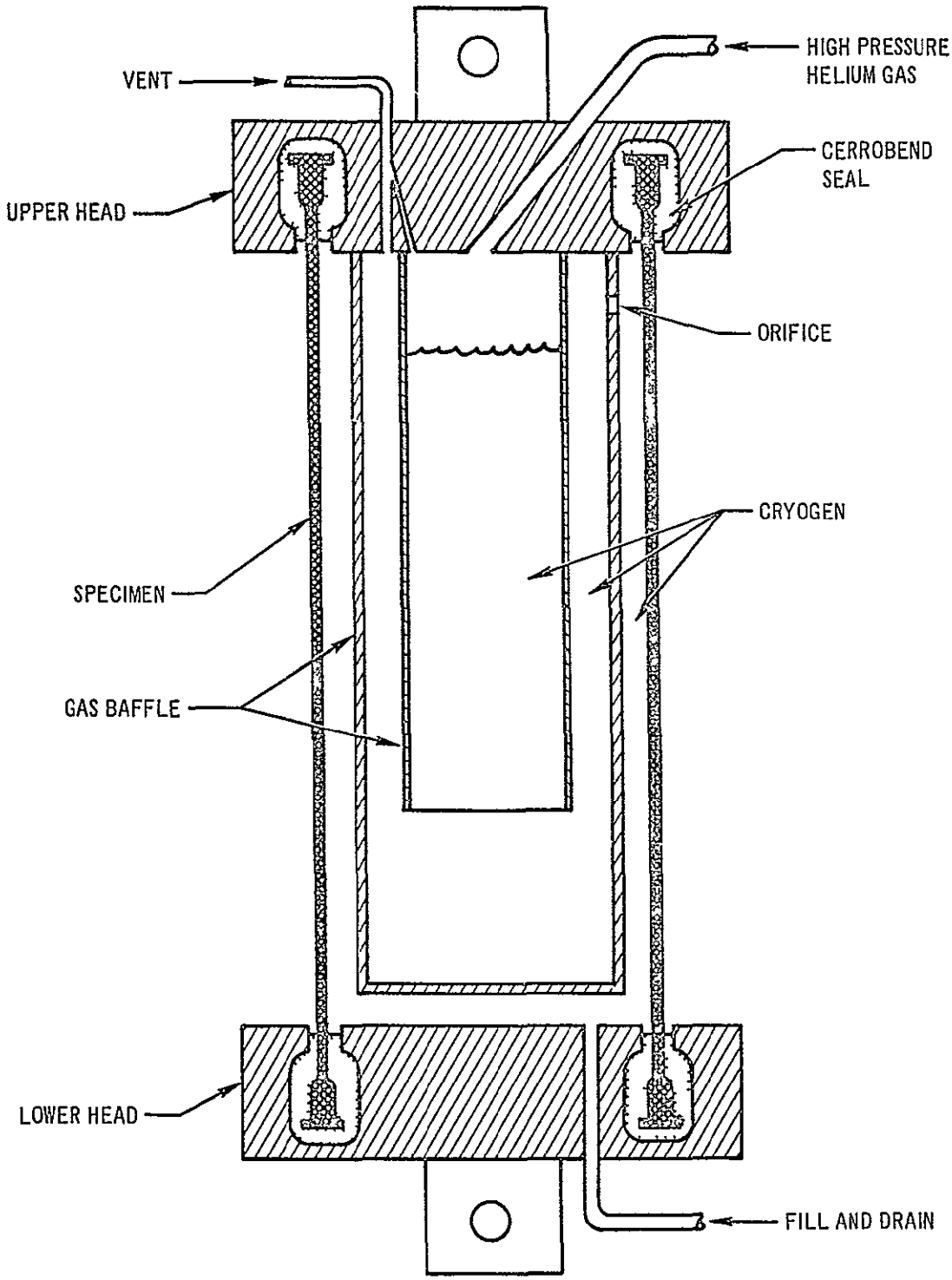

Figure 6 Biaxial Specimen Assembly for Cryogenic Tests

pressurize the test cylinders The specimen loading ratio was controlled manually by following an appropriate X-Y recorder plot of Baldwin machine hydraulic pressure versus specimen pressure The X-Y recorder plot was devised to provide a 2-to-1 or a 1-to-1 (axial-to-hoop) biaxial stress ratio

Remaining room temperature and all cryogenic biaxial tests were performed in a special test machine (P/N 1T06601-1) The test machine consisted of a system for applying the desired stress ratios to the cylindrical specimens by means of a single high pressure gas source Prior to pressurization, the specimens were filled with water for room temperature tests and with liquid nitrogen or liquid hydrogen for the cryogenic tests In all cryogenic tests the specimens were submerged in liquid nitrogen or liquid hydrogen contained in a cylindrical cryostat Specimens were pressurized using gaseous nitrogen at room temperature and gaseous helium at cryogenic temperatures

Instrumentation

For the purpose of detecting the formation of cracks in the welds of the loaded specimens prior to bursting, crack wires (44-gage insulated Formvar) were bonded to the welds and connected to the recording equipment, a wire failure was therefore synchronized with specimen pressure

For room temperature tests, the 2-to-1 (axial-to-hoop) specimens were equipped with two crack wires installed on one of the two longitudinal welds as shown in Figure 7 For cryogenic tests, both longitudinal welds in the 2-to-1 (axial-to-hoop) specimens were equipped with two crack wires

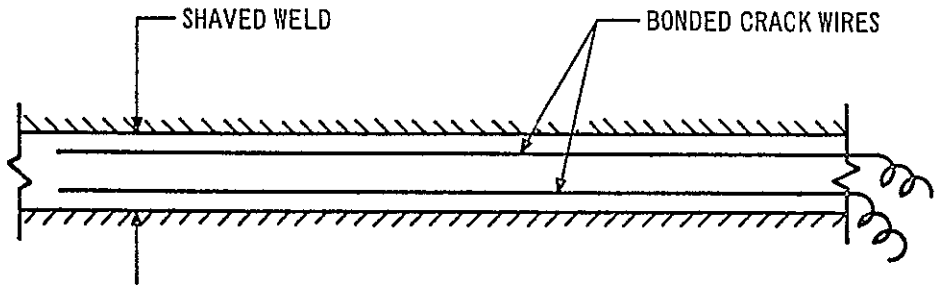

a |2-TO-1 (AXIAL-TO-HOOP) CONFIGURATION

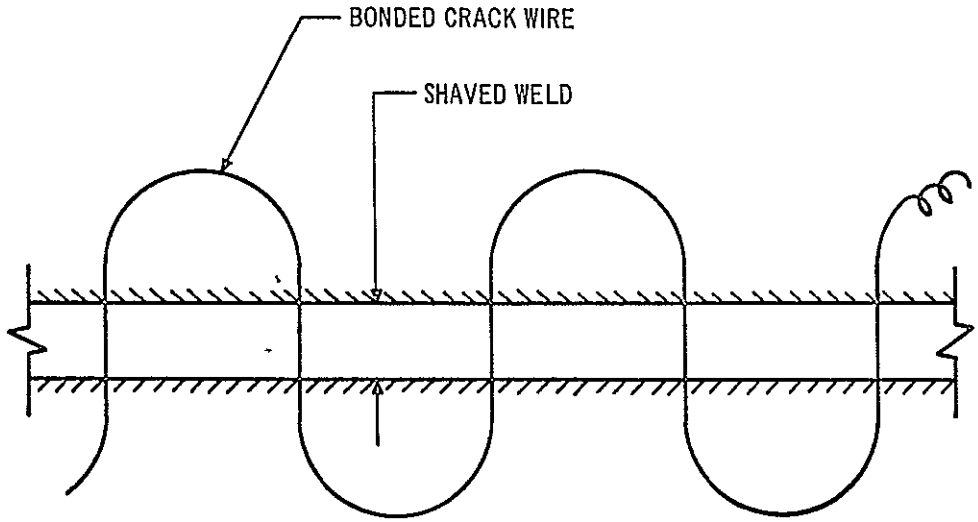

b 1-TO-1 (AXIAL-TO-HOOP) CONFIGURATION

Figure 7 Schematic Installation of Crack Wires on Longitudinal Welds of Cylinders

For the 1-to-1 (axial-to-hoop) specimens, crack wires were laid in the form of a sine wave crossing the weld Two acoustical methods for detection of crack formation were attempted The first method involved the attachment to the specimen of a crystal accelerometer which was connected to an oscillograph, ear phones and a tape recorder Background noise prevented the successful use of this method The second method, also unsuccessful due to excessive noise, involved the use of six crystal accelerometers to detect and locate cracks by triangulation This method was supervised by an Aerojet-General representative, as requested by NASA

All specimens were equipped with at least one biaxial strain gage mounted either on the parent metal or on the weld to monitor the stress state On some specimens, biaxial strain gages were located back-to-back on the weld and on the parent metal Certain specimens were instrumented with deflection transducers to measure circumferential growth at the center of the specimen

Specimen internal pressure and axial load (in terms of pressure) as detected by electrical pressure transducers were recorded for all tests on an X-Y recorder Internal pressure was also monitored by a mechanical bourdon-type dial gage All electrical pressure gage, crack wire and strain gage outputs were recorded on an oscillograph or by the Digital Data System

Two specimens were instrumented for the purpose of evaluating stress distribution along the weld during loading at room temperature Photo-stress was applied to the weld of specimen B1 and back-to-back biaxial strain gages were located approximately 8 inches from the doublers at

one end of specimen B4. Specimen B1 was first pressurized to produce a 1-to-2 (axial-to-hoop) stress state, this pressure was maintained while the axial load was increased to produce a 2-to-1 (axial-to-hoop) stress state This loading procedure was followed several times and photographs of the stress patterns were taken for analysis

Test Procedures

Assembled room temperature test specimens were installed in either of the two test machines, filled with water and pressurized and axially loaded in steps up to a longitudinal stress of 55 ksi for the 2-to-1 (axial-to-hoop) specimens and 24 ksi for the 1-to-1 (axial-to-hoop) specimens After each loading step, the one longitudinal weld not equipped with crack wires was dye checked for cracks After achieving the above stress levels, the specimen pressurization and axial loading were applied continuously to failure

Specimens for -320°F tests were first purged with helium gas After purging, the specimens were pressurized with helium gas at 75 psig to maintain positive internal pressure during filling of the cryostat with liquid nitrogen Upon completion of the cryostat fill, specimens were filled with liquid nitrogen and permitted to stabilize at -320°F An instrumentation zero was taken and, with recording equipment operating, helium gas pressure (internal and axial load) was applied continuously until failure.

The procedure for -423°F tests was similar Specimens were purged with helium gas and pressurized at 75 psig during a pre-chilling operation in which the cryostat was filled with liquid nitrogen The cryostat was

purged with helium gas after draining of the liquid nitrogen Specimens were pressurized with helium at 75 psig during filling of the cryostat with liquid hydrogen. The specimens were then filled with liquid hydrogen and allowed to stabilize at -423°F An instrumentation zero was taken and helium gas pressure (internal and axial load) applied continuously until failure occurred

Failure Analysis

A metallurgical examination was performed on each biaxial specimen after bursting Parent and weld metal tensile tests were performed on uniaxial tensile specimens machined from the cylinder trim as shown in Figure 8 Specimen dimensions are given in Figure 9

The fracture path of each failed biaxial specimen was mapped An attempt, using visual or electron fractography, was made to locate the origin of each failure The map of the fracture and the location of the origin, if determined, were compared with dimensional and quality data obtained on each specimen prior to testing Metallographic specimens of selected areas were made and examined The unfailed portions of some welds were subjected to radiographic and dye penetrant inspection in an attempt to discover cracks caused by the testing

Methods of Analysis

Biaxial Strength

For essentially homogeneous structures, most combinations of biaxial tension stresses result in observed biaxial yield and ultimate strengths higher than corresponding uniaxial strengths, for the 1-to-1 stress state, in which the

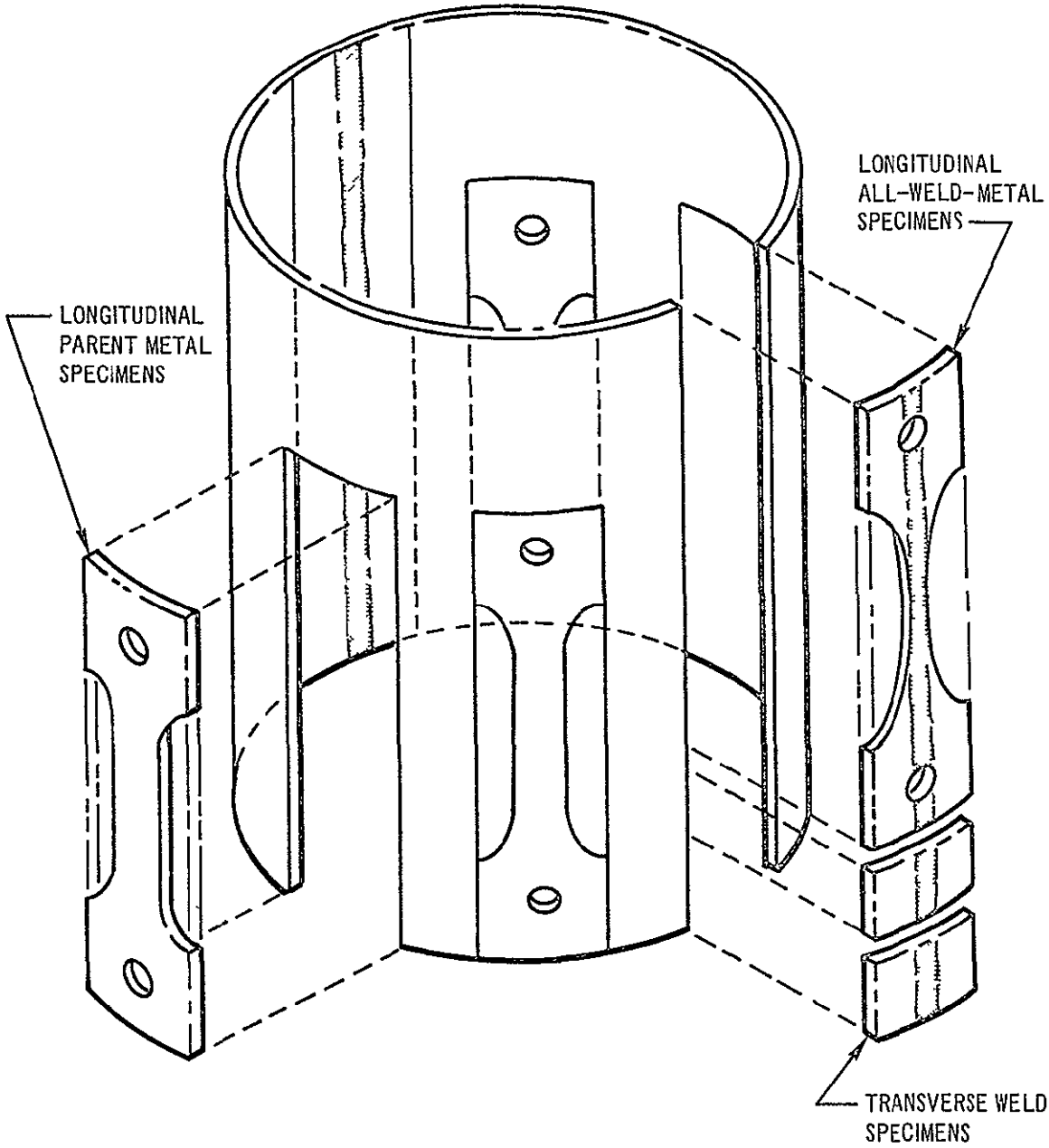

Figure 8 Tensile Specimens Machined from Cylinder Trim

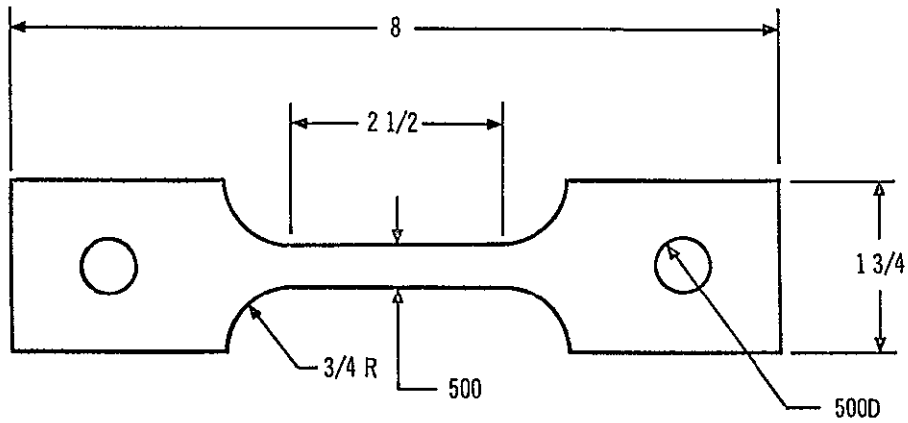

PARENT METAL TENSILE

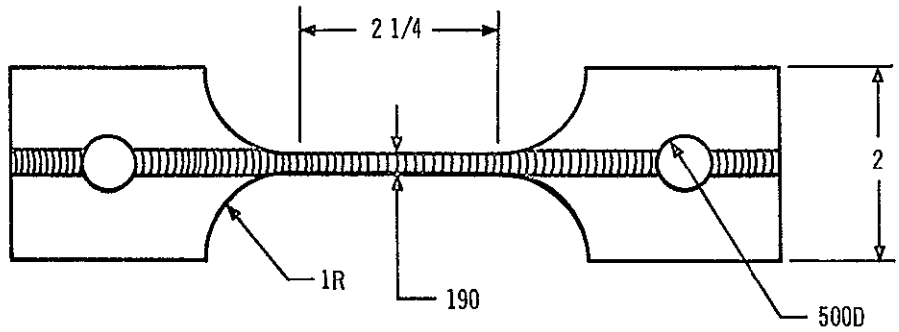

LONGITUDINAL ALL-WELD-METAL TENSILE

DIMENSIONS ARE IN INCHES

Figure 9 Tensile Specimen Dimensions

two principal stresses are equal, biaxial strengths are equal to uniaxial strengths

Various theoretical treatments (References 2, 3) are available which give the biaxial yield strength as a function of stress state Others, (References 4, 5) have shown that biaxial ultimate strength (plastic instability stress) can also be treated theoretically The biaxial plastic-instability-stress envelope for titanium alloys was shown (Reference 6) to conform with Hill's description of the biaxial yield strength envelope for anisotropic materials (Reference 7) Using Hill's model, the biaxial strength can be described by the expression

$$\sigma_A^2 - 2\left(\frac{R}{R+1}\right)\sigma_A\,\sigma_H + \sigma_H^2 = \sigma_u^2 \qquad (1)$$

where

σ_A = axial stress at failure

σ_H = hoop stress at failure

σ_u = uniaxial ultimate strength

R = a parameter equal to the ratio of lateral-to-thickness strain in a pure uniaxial stress state

The parameter, R, is equal to 1 0 for isotropic materials, such as 2014-T6

For isotropic materials Eq 1 therefore reduces to

$$\sigma_A^2 - \sigma_A\,\sigma_H + \sigma_H^2 = \sigma_u^2 \qquad (2)$$

Figure 10 illustrates the biaxial strength envelope for all tensile stress states for a homogeneous, isotropic structure, as predicted from Eq 2

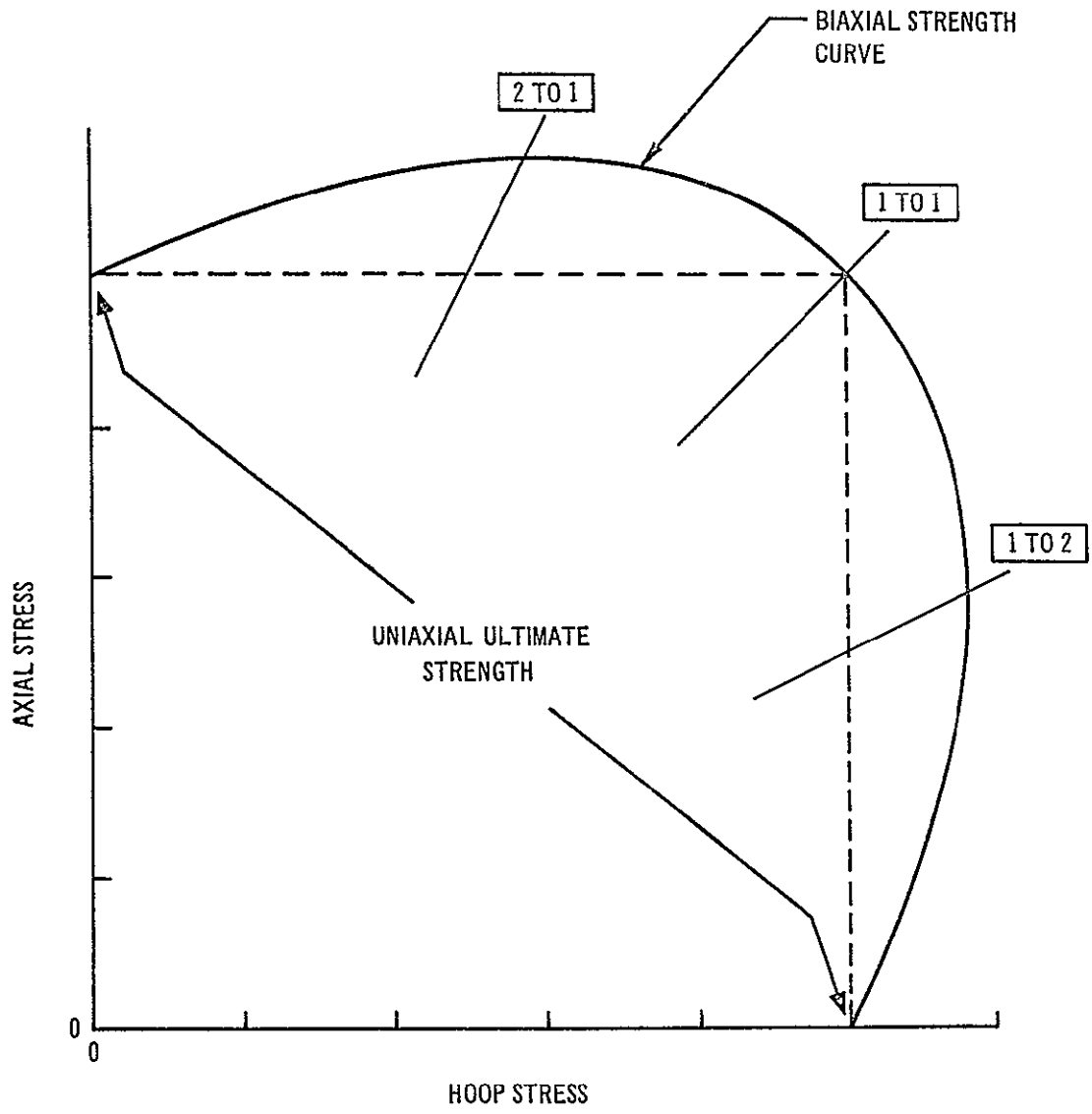

Figure 10 Biaxial Strength Envelope for a Homogeneous Isotropic Structure

In a non-homogeneous structure, in which the strength may vary from place to place in the structure due to the presence of welds, geometrical discontinuities and the like, the strength envelope for biaxial tension stress states is less straightforward The welded 2014 cylinder tested in this program is such a non-homogeneous structure since it contains two longitudinal weldments having strengths considerably less than the adjacent parent metal

Development of Biaxial Strength Envelope

Only two biaxial stress states were evaluated in this program Nevertheless, for most test conditions the shape of the biaxial ultimate strength envelope can be developed First of all, the intersection of the envelope curve with the vertical (axial stress) coordinate represents a 1-to-0 stress state in which a cylinder is axially loaded only and the hoop stress therefore is zero The location of this point on the stress coordinate can be inferred from the results of uniaxial tests of flat panels containing a longitudinal (parallel with the loading direction) weld. As long as the entire system remains elastic, the axial stress in the parent metal equals the axial stress in the longitudinal weld regardless of minor differences in thickness (assuming that the strain and modulus are equal in parent metal and weld) as shown in Figure 11, Point A At higher axial loads where the strains are such that the stress in the weld exceeds the proportional limit of the weld, the stress in the parent metal exceeds the stress in the weld (Point B in Figure 11) If the ductility of the weld metal is such that the weld can continue straining until the stress in the parent metal reaches parent metal ultimate tensile strength, then the strength of the panel is

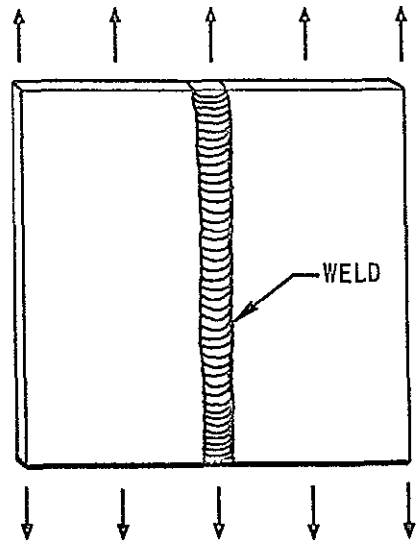

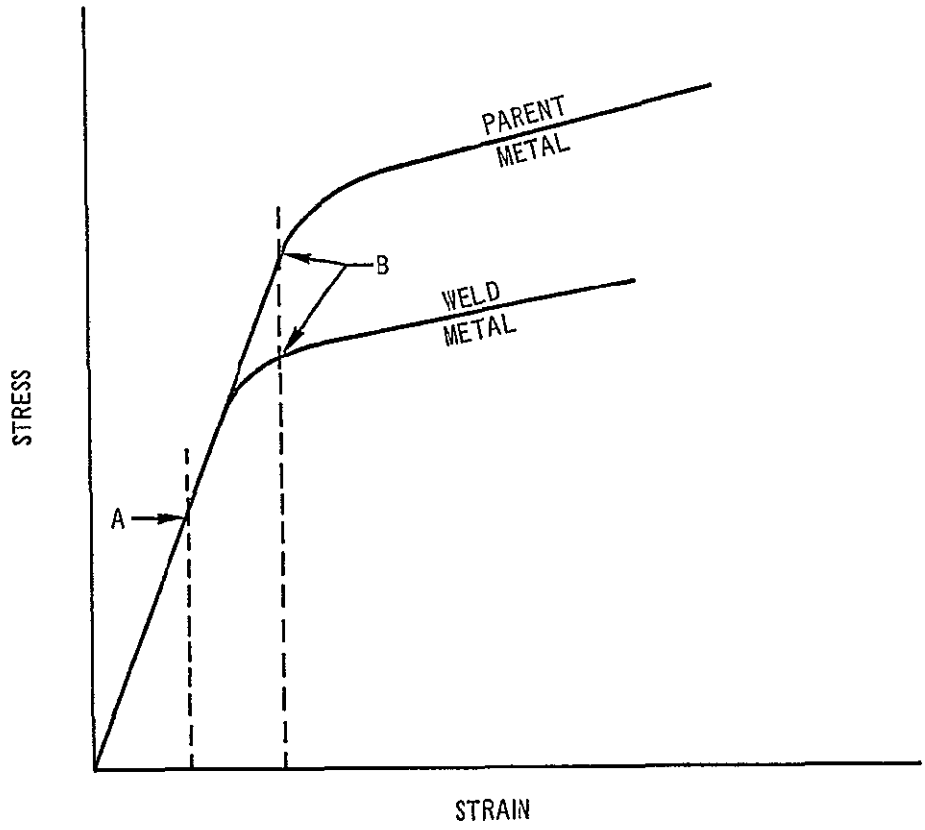

Figure 11 Uniform Strain and Non–Uniform Stress in a Non–Homogeneous Panel

$$\sigma\,(\text{panel}) = \sigma\,(\text{P M}) - \frac{W\,(\text{weld})}{W\,(\text{panel})}\left[\sigma\,(\text{P M}) - \sigma\,(\text{weld})\right] \qquad (3)$$

where $\sigma\,(\text{panel})$ = Strength of panel

$\sigma\,(\text{P M})$ = Strength of parent metal

$\sigma\,(\text{weld})$ = Strength of weld (longitudinal all weld metal)

$W\,(\text{weld})$ = Width of weld

$W\,(\text{panel})$ = Width of panel

Table 4 illustrates the ability of Eq 3 to describe panel strength for various width panels of 2014-T6 containing longitudinal MIG welds subjected to a double cure cycle after welding (Reference 8) Tests were performed at room temperature and each strength value represents an average of three tests

The analogous equation for the uniaxial strength of a longitudinally welded cylinder is·

$$\sigma\,(\text{cyl}) = \sigma\,(\text{P M}) - \frac{W\,(\text{weld})}{\pi D}\left[\sigma\,(\text{P M}) - \sigma\,(\text{weld})\right] \qquad (4)$$

where $\sigma\,(\text{cyl})$ = Axial strength of cylinder (1-to-0)

D = Diameter of cylinder

The intersection of the strength envelope curve with the horizontal (hoop stress) axis represents a 0-to-1 stress state in which a cylinder is loaded in the hoop direction only and the axial stress therefore is zero Failure of a cylinder loaded in this manner will occur when the

TABLE 4

COMPARISON OF CALCULATED AND MEASURED COMPOSITE STRENGTHS OF LONGITUDINALLY WELDED PANELS

Width of Panel in	Width of Weld in	Width of Parent Metal in	Strength of Weld ksi	Strength of Parent Metal ksi	Calculated Composite Strength of Panel (1) ksi	Measured Composite Strength of Panel ksi
200	200	0	46 7	70 0	46 7	46 7
1 5	300	1 25	46 7	70 0	65 3	65 5
2 5	300	2 25	46 7	70.0	67 1	66 9
4.0	.300	3 75	46 7	70 0	68 0	67 5

(1) Calculated using Eq. 3.

hoop stress reaches the uniaxial transverse weld strength, if there is no difference in parent metal and weld thickness The location of this point on the hoop stress coordinate can therefore be inferred from uniaxial tests of flat panels containing a weld perpendicular to the loading direction

Figure 12 illustrates the developed biaxial strength envelope for a cylinder containing two longitudinal welds For this example the longitudinal and transverse weld strengths were taken both as 66% of parent metal strength

Failure Control

The strength envelope indicates that in a biaxial burst test, failure will be controlled by either the transverse weld strength or the longitudinal cylinder (essentially parent metal) strength depending on the stress state If the stress state is in the region 1-to-0 to about 1 5-to-1, failure is controlled by the longitudinal cylinder strength If the stress state is in the region of about 1 5-to-1 to .0-to-1, failure is controlled by the transverse weld strength

The relationship between stress state and failure control can be generalized if stress state is expressed as a fraction as

$$\text{Stress State} = \frac{\text{axial stress}}{\text{hoop stress}} = K \qquad (5)$$

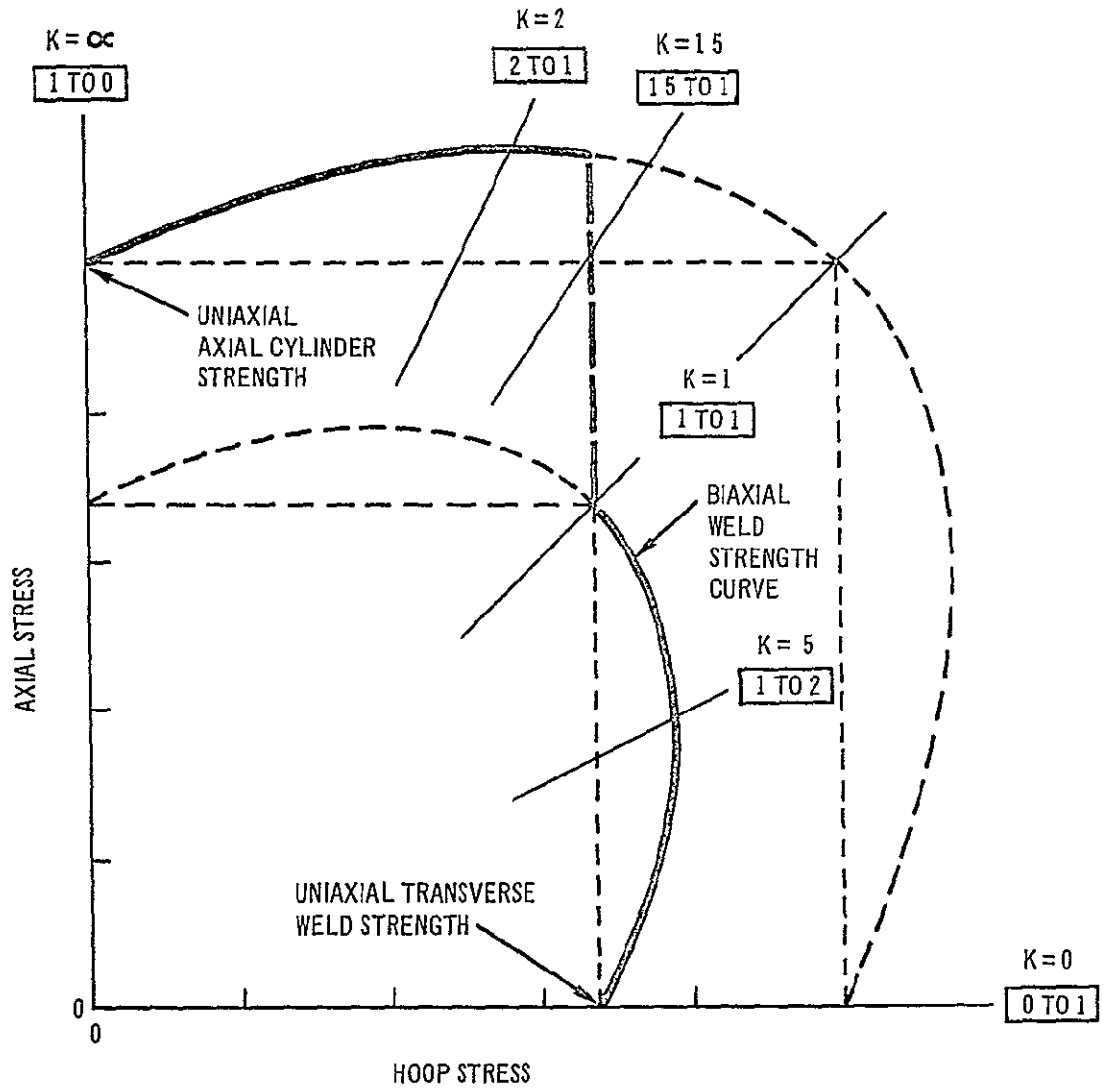

Figure 12 Biaxial Strength Envelope for Cylinder (Non–Homogeneous Isotropic) Containing Two Longitudinal Welds

Then stress states of 1-to-0, 2-to-1, 1-to-1 and 0-to-1 are expressed as ∞, 2, 1, and 0 The longitudinal cylinder strength controls failure in the range of stress states ∞ to K*, where

$$(K^*)^2 - K^* + 1 = \frac{(\text{long cylinder strength})^2}{(\text{trans weld strength})^2} \qquad (6)$$

where the strengths are uniaxial values Transverse weld strength controls failure in the range of stress states K* to 0

Strain Limitations

The shape of the biaxial strength envelope depends to some degree upon the ability of the weld to strain without rupturing If the longitudinal weld in a cylinder stressed 2-to-1 (axial-to-hoop) reaches the limit of its ability to strain in the axial direction before the parent metal axial stress reaches ultimate (biaxial) strength, then the weld will crack first The crack will form across the longitudinal weld normal to the maximum (axial) strain direction It is likely that the weld crack will extend at least from one fusion line to the other (and possibly into the heat-affected zones on either side of the weld) It is also likely that the crack will exist completely through the thickness of the weld fusion zone from the I D of the cylinder to the O D

If the resistance of the parent metal to the presence of such a through crack is such that the crack is arrested, a small leak can occur but the cylinder will not fail by fracturing until the stress is increased to some higher level In the case of an axially loaded cylinder, the leak does not prevent further axial loading and the axial stress could be

increased to the point of fracture In a pressure vessel, the leak may be of sufficient magnitude that a further pressure increase is not possible and fracture could not occur

If the resistance of the parent metal to the presence of the through crack is such that the crack is not arrested, fracture of the cylinder will occur immediately with no further increase in stress The biaxial strength of the cylinder under these conditions would be less than predicted

Figure 13 illustrates conditions under which leak-before-fracture and fracture-before-leak could occur The curve represents the axial strength of a cylinder as a function of the length of a through crack normal to the axial stress If the weld crack due to the limiting strain capability of the weld is short enough, the cylinder can be stressed axially to its ultimate strength regardless of when the weld crack forms. If the weld crack is somewhat longer, however, the axial strength of the cylinder can be reduced. The actual reduction depends on when the crack forms If the crack forms at a low axial stress, the cylinder can be loaded until the axial stress is equal to the fracture strength characteristic of the length of the crack If the crack does not form until the axial stress has reached a level above the characteristic fracture strength, then fracture will occur immediately and the reduction in cylinder strength will be somewhat less

The elastic axial fracture stress of a cylinder can be determined (Reference 9) from:

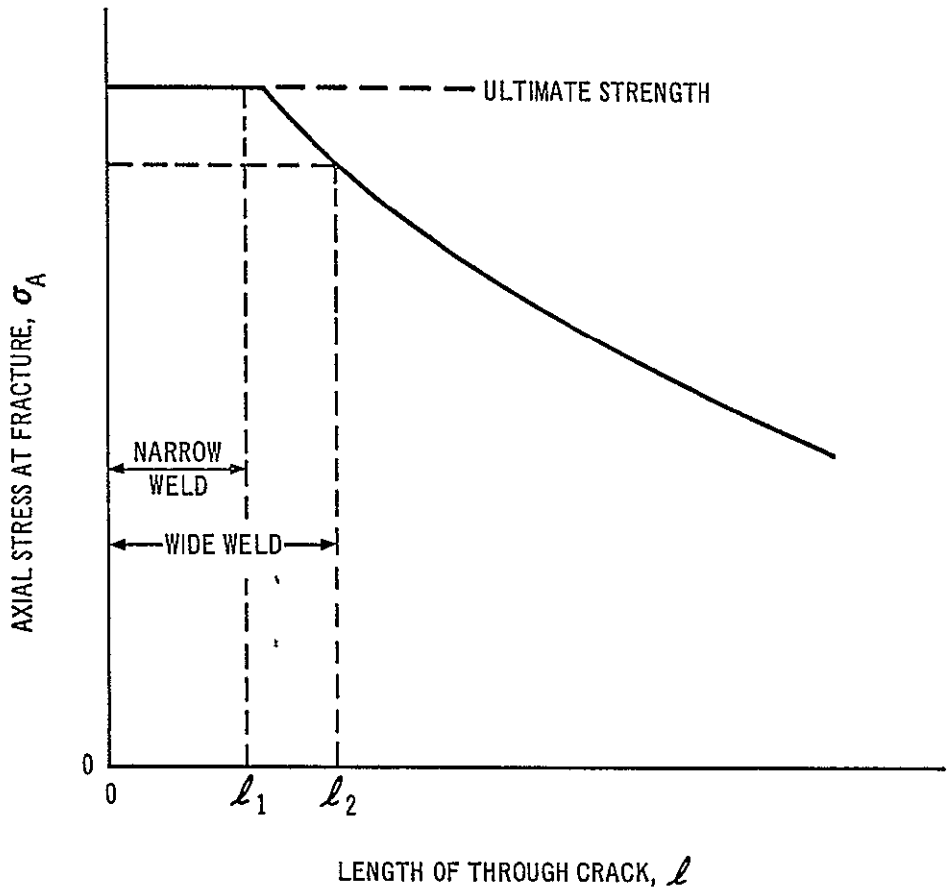

Figure 13 Effect of Transverse Cracks in Longitudinal Welds on Residual Axial Strength of Cylinder

$$\sigma_A^2 = \frac{K_c^2}{\pi\left[\frac{\ell}{2} + \frac{1}{2\pi}\left(\frac{K_c}{\sigma_y}\right)^2\right]} \qquad (7)$$

where σ_A = axial fracture stress

K_c = plane-stress stress intensity of parent metal

ℓ = length of through crack

σ_y = yield strength (biaxial) of parent metal

Equation 7 is not valid at axial stresses above yield strength For the case of weld strain limitation, the length of crack, ℓ, can be taken as that width of the weld and heat-affected zone which rupture (effective width of weld)

The biaxial strength envelope for a cylinder with longitudinal weld strain limitation leading to low stress fracture is truncated in the region of high axial stresses If a weld crack occurs at some value of axial stress less than the biaxial ultimate, the strength envelope is truncated at the failure stress for the cylinder characteristic of a through crack equal in length to the effective width of weld The truncated biaxial strength envelope for a case of longitudinal weld strain limitation is shown in Figure 14 The figure is based on the data in Figure 12

RESULTS

Detailed measurements made in all biaxial tests, including strain gage, deflection gage and transducer readouts are given in Reference 1

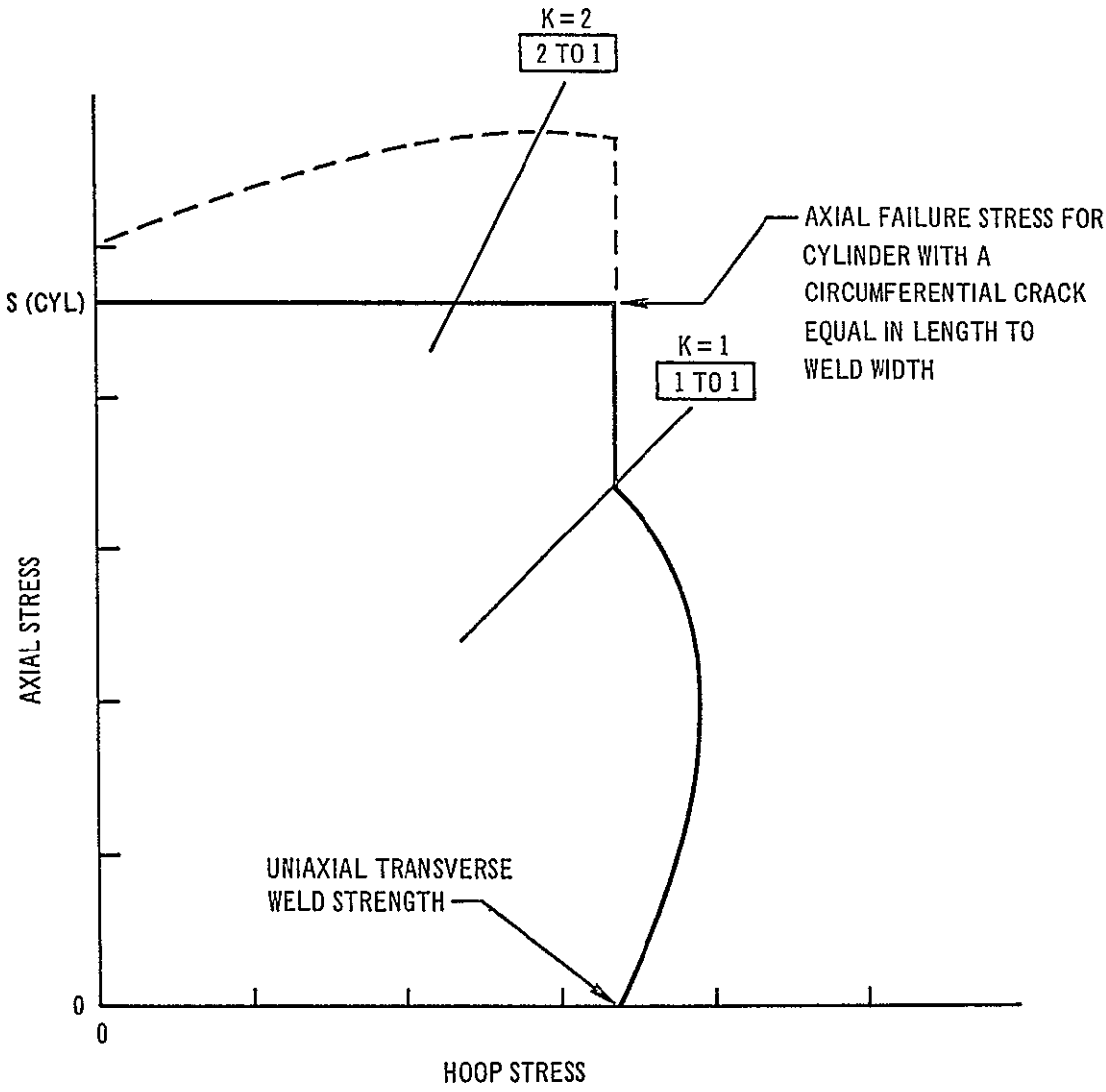

Figure 14 Truncated Biaxial Strength Envelope for a Cylinder Exhibiting Strain Limitation in Longitudinal Weld

Stress State and Distribution

Specimen B1 with photostress applied to one of the longitudinal welds showed a uniform stress distribution along the weld and indicated that end effects due to the loading heads were negligible Furthermore, the biaxial strain gages installed on specimen B4 showed nearly the same biaxial stress ratio as the gages located at the center of the specimen

Biaxial Test Results

Nominal axial and hoop stresses in the parent metal at the time of first weld crack indication and at burst for all biaxial tests are given in Tables 5 through 9 In the tables both the test code number and the production code number of each specimen are listed for reference The stresses were calculated using the average parent metal thickness in the circumferential section near the fracture (2-to-1, axial-to-hoop, tests) or the average parent metal thickness adjacent and parallel to the weld (1-to-1, axial-to-hoop, tests) Thicknesses as measured prior to testing were employed in these calculations

For some specimens there was no indication of weld cracking prior to bursting In tests at 70° and -320°F, 15 out of 36 specimens tested gave indications of cracking prior to burst In the six tests at -423°F, no cracking prior to burst was indicated

TABLE 5

RESULTS OF 2-TO-1 BIAXIAL TESTS AT 70°F

Type Weld	Specimen Code		First Crack Indication, Stress		Burst		Burst Stress (1)		Failure Analysis Report No
	Test	Prod	Axial ksi	Hoop ksi	Axial Load lbs	Internal Pressure psig	Axial ksi	Hoop ksi	
NO CURE									
MIG	A1	A1	76 6	38 3	303,500	505	77 0	38 5	MP 20,425
	B1	B1	77 4	39 2	302,000	510	77.8	39 4	MP 20,426
	C4	C4	(2)	(2)	350,000	420	75 1	37 8	MP 20,435
TIG	J1	J3	(2)	(2)	308,000	510	77 8	38 8	MP 20,477
	J2	E3	76 2	37 1	308,000	510	78 3	39 2	MP 20,477
	J3	D1	77 6	38 6	315,000	521	77.0	38 5	MP 20,477
CURED									
MIG	B3	B3	(2)	(2)	332,000	470	73 3	36 7	MP 20,473
	B4	B4	(2)	(2)	288,500	485	74 3	37 3	MP 20,444
	C1	C1	72 5	36 2	302,500	503	76 3	38 2	MP 20,455
TIG	D2	01	(2)	(2)	319,000	527	81 6	40 7	MP 20,452
	D3	02	(2)	(2)	316,000	523	81 7	40 7	MP 20,453
	D4	P1	(2)	(2)	323,000	535	80 6	40 5	MP 20,449

(1) Stress based on average parent metal thickness in the circumferential section at the failure location

(2) No indication of crack prior to burst

TABLE 6

RESULTS OF 2-TO-1 BIAXIAL TESTS AT -320°F

Type Weld	Specimen Code		First Crack Indication, Stress		Burst		Burst Stress (1)		Failure Analysis Report No
	Test	Prod	Axial ksi	Hoop ksi	Axial Load lbs	Internal Pressure psig	Axial ksi	Hoop ksi	
NO CURE									
MIG	F2	L3	(2)	(2)	363,000	603	91 5	45 7	MP 20,451
	F3	H1	(2)	(2)	331,000	547	85 0	42 5	MP 20,451
	G4	K3	85 0	42 5	345,000	570	87 2	43 6	MP 20,496
TIG	L2	M1	(2)	(2)	345,000	570	86 9	43 2	MP 20,459
	K4S	M2	87 7	43 8	375,000	620	88 2	44 1	(3)
	L1S	H3	84 5	42 2	353,000	583	89 0	45 0	MP 20,485
CURED									
MIG	C2	C2	77 2	38 6	353,000	585	90 9	45 1	MP 20,454
	E2	N1	(2)	(2)	270,000	447	70 3	35 0	(4)
	H2	Q3	(2)	(2)	326,500	540	85 6	42 8	MP 20,494
TIG	E3	F2	(2)	(2)	349,000	578	88 9	44 3	MP 20,470
	E4	I1	(2)	(2)	336,000	555	83 7	41 8	MP 20,470
	F1	Q1	(2)	(2)	318,000	525	80 2	40 1	MP 20,451

(1) Stress based on average parent metal thickness in the circumferential section at the failure location

(2) No indication of crack prior to burst

(3) No failure report written

(4) Report number not yet assigned

TABLE 7

RESULTS OF 2-TO-1 BIAXIAL TESTS AT -423°F

Type Weld	Specimen Code		First Crack Indication, Stress		Burst		Burst Stress (1)		Failure Analysis Report Number
	Test	Prod	Axial ksi	Hoop ksi	Axial Load lbs	Internal Pressure psig	Axial ksi	Hoop ksi	
NO CURE									
MIG	H3	R3	(2)	(2)	326,000	539	81 5	40 7	(3)
	H4	Q2	(2)	(2)	324,000	535	81 6	40 7	(3)
	I1	P2	(2)	(2)	309,000	511	77 0	38 5	(3)
TIG	I2	J2	(2)	(2)	330,000	545	83 7	41 8	MP 50,020
	I3	E1	(2)	(2)	350,000	578	88 2	44 1	MP 50,020
	I4	T1	(2)	(2)	354,000	585	91 2	45 7	MP 50,020

(1) Stress based on average parent metal thickness in the circumferential section at the failure location

(2) No indication of crack prior to burst

(3) Report number not yet assigned

TABLE 8

RESULTS OF 1-TO-1 BIAXIAL TESTS AT 70°F

Type Weld	Specimen Code		First Crack Indication, Stress		Burst		Burst Stress (1)		Failure Analysis Report Number
	Test	Prod.	Axial ksi	Hoop ksi	Axial Load lbs	Internal Pressure psig	Axial ksi	Hoop ksi	
NO CURE									
MIG	C3	C3	48 3	48.3	128,000	630	49 3	49 2	MP 20,443
	B2	B2	(2)	(2)	125,000	617	47 4	47 1	MP 20,434
	D1	L2	(2)	(2)	132,000	642	49 9	48 4	MP 20,474
TIG	J4	H2	48 1	48 1	126,500	625	48 9	48.9	MP 20,469
	K1	K1	45 7	45.7	123,000	608	46 5	46 5	MP 20,469
	K2	K2	(2)	(2)	123,500	612	47 1	47 1	MP 20,469

(1) Stress based on average parent metal thickness adjacent and parallel to the weld

(2) No indication of crack prior to burst.

TABLE 9

RESULTS OF 1-TO-1 BIAXIAL TESTS AT -320°F

Type Weld	Specimen Code		First Crack Indication, Stress		Burst		Burst Stress (1)		Failure Analysis Report Number
	Test	Prod	Axial ksi	Hoop ksi	Axial Load lbs.	Internal Pressure psig	Axial ksi	Hoop ksi	
NO CURE									
MIG	G2	G2	(2)	(2)	127,500	630	48.3	48 3	MP 20,495
	G3	J1	(2)	(2)	129,000	638	49 1	49 1	MP 20,495
	H1	F3	49.6	49 6	137,000	679	53 8	53 8	MP 20,495
TIG	K35	M3	(2)	(2)	136,500	675	54 0	54 0	MP 20,486
	L3	U3	53 4	53 4	148,000	735	57 1	57 1	MP 20,486
	L4	S1	55 8	55 8	147,500	730	58.4	58 4	MP 20,486

(1) Stress based on average parent metal thickness adjacent and parallel to the weld

(2) No indication of crack prior to burst.

Failure Analysis

Two fracture orientations were evident in the failed specimens As shown in Figure 15, cylinders subjected to a 2-to-1 (axial-to-hoop) stress state exhibited a circumferential fracture lying essentially in a plane normal to the maximum (axial) stress Cylinders tested in a 1-to-1 (axial-to-hoop) stress state exhibited an axial fracture lying in or adjacent to the weld as shown in Figure 16 Secondary fracturing occurred in several cylinders

In the circumferential (2-to-1 stress state) fractures sufficient fractographic evidence was usually available to permit locating the fracture origin in one of the two longitudinal welds In the axial fractures, however, location of a fracture origin was usually not possible due to the lack of distinguishing fractographic evidence in the failed weld metal In all cases in which the location of the fracture origin could be determined no evidence of prior defects in the vicinity of the origin could be found Some welds contained radiographically acceptable porosity but this type of prior defect was never located at established fracture origins In two cylinders surface defects in the parent metal (vibrotool marks and a scratch) influenced the direction of the fracture but were not associated with the fracture origin

No unusual microstructural features were observed in metallographic samples taken from fracture origins or along fracture paths

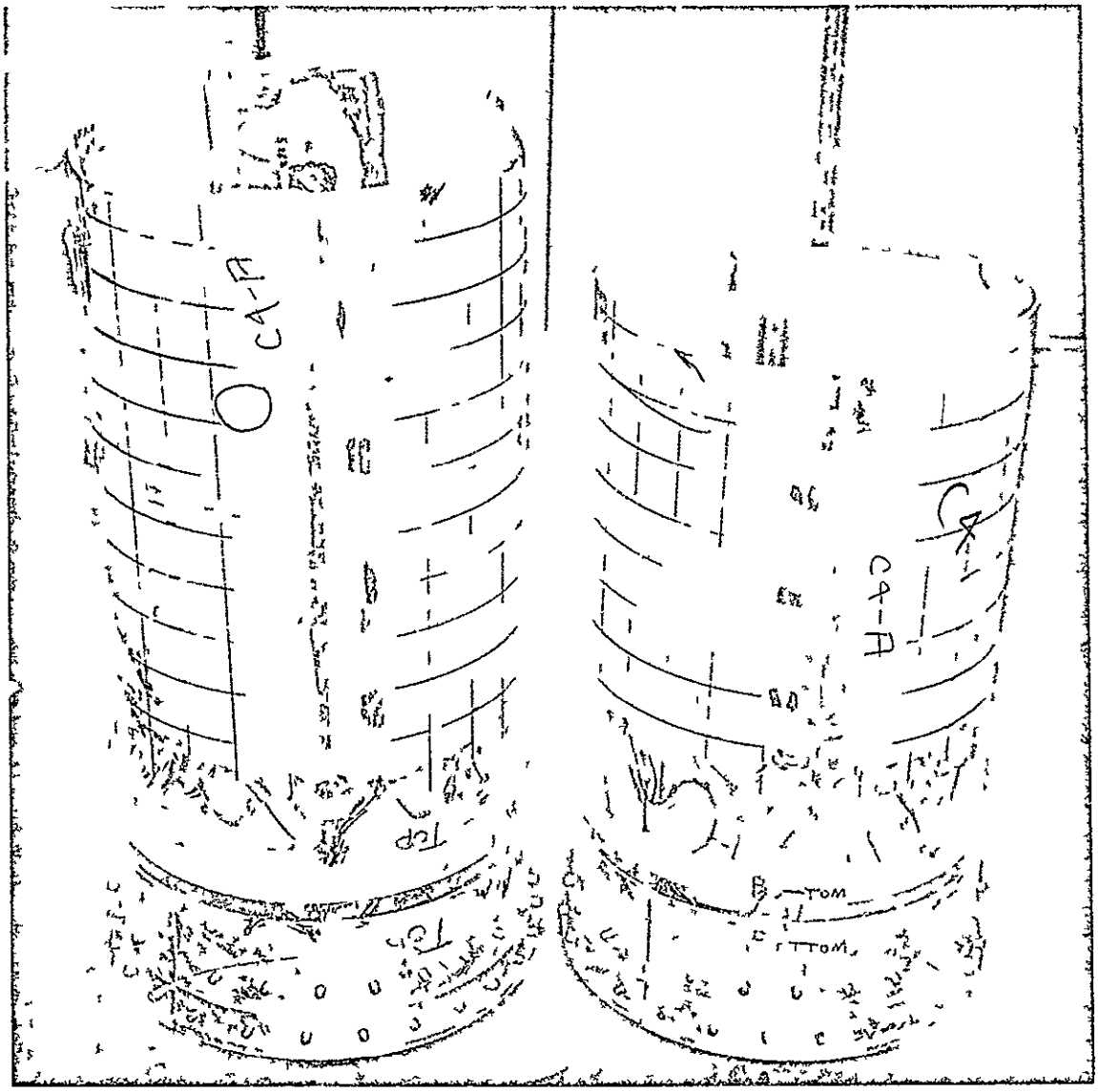

SM 439578

Figure 15 Specimen C4 after 2–to–1 (Axial–to–Hoop) Biaxial Test at 70°F Illustrating Circumferential Fracture

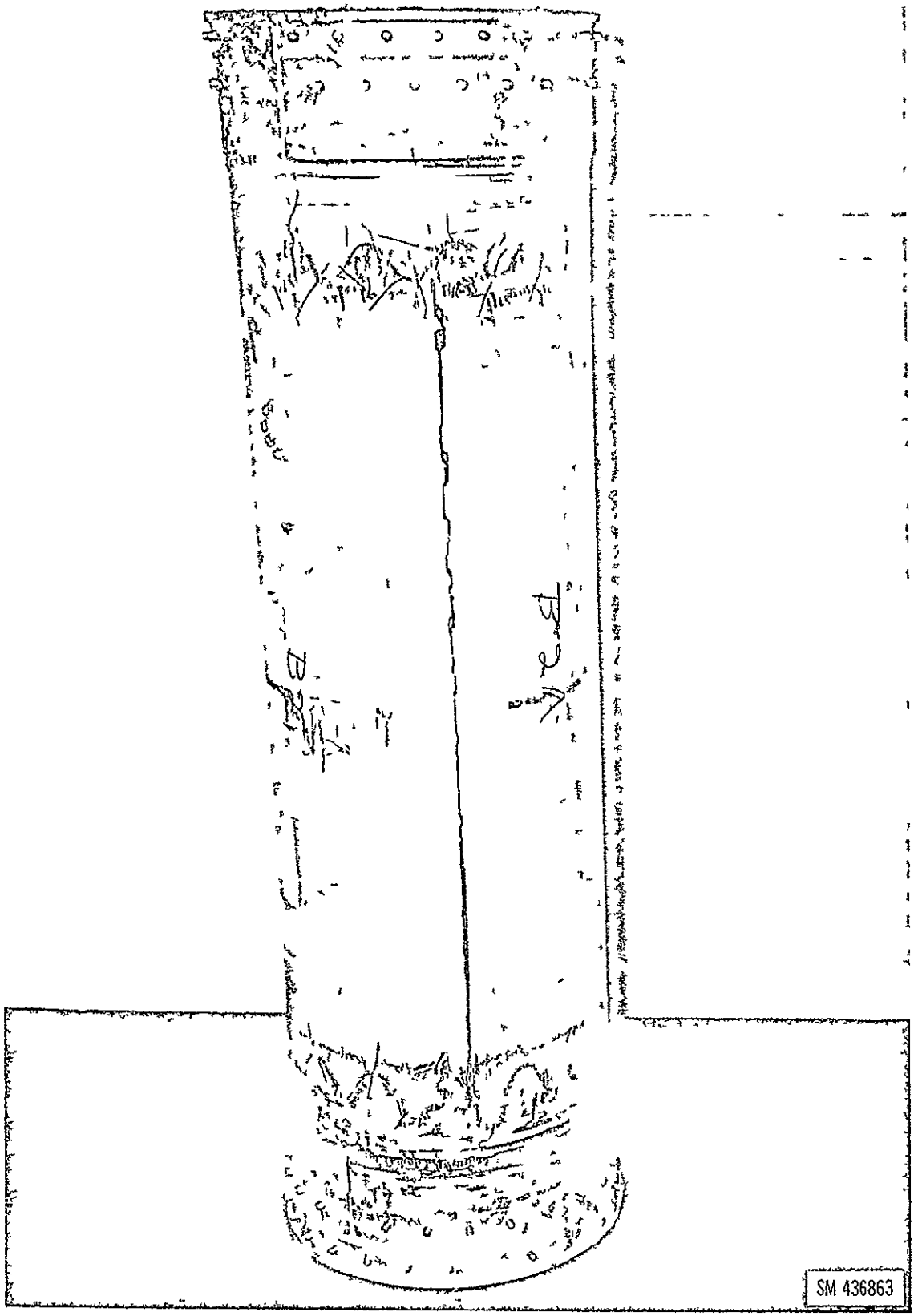

Figure 16 Specimen B2 after 1–to–1 (Axial–to–Hoop) Biaxial Test at 70°F Illustrating Axial Fracture

Radiographic and dye penetrant inspection of unfailed portions of two cylinders (test Code A1 and B1) tested at 70°F in a 2-to-1 (axial-to-hoop) stress state revealed the presence of shallow surface cracks oriented normal to the maximum (axial) stress Both cylinders gave indications of cracks prior to burst during the biaxial test In specimen B1, the cracking was located in the heat-affected zone on the O D surface (Figure 17) and in the fusion zone on the I D surface of both longitudinal welds Figure 18 is a metallographic section of typical surface cracks in B1 In specimen A1, the cracking was confined to the heat-affected zone on the O D surface The original inspection records of both cylinders contained no evidence that the surface cracks existed prior to biaxial testing

The results of uniaxial tests performed on coupons removed from the cylinder trim of each biaxial specimen are presented in Tables 10 - 13 Under all comparable uniaxial test conditions, TIG welds exhibited higher yield strength, ultimate strength and elongation than MIG welds The following effects due to curing were observed

a Yield and ultimate strengths of parent metal were not affected, but a trend toward slightly reduced elongation due to curing was noted,

b. In all-weld-metal tensile coupons tested at 70°F and -320°F, curing resulted in an increase of approximately 50% in yield strength and 10% in ultimate strength while elongation was reduced approximately 50%,

TABLE 10

AVERAGE UNIAXIAL TENSILE PROPERTIES OBTAINED FROM CONTROL COUPONS TAKEN FROM UNCURED MIG-WELDED CYLINDER TRIM

Biaxial Specimen Code		Test Temp °F	UNIAXIAL PROPERTIES							
			PARENT METAL (1)			LONGITUDINAL ALL-WELD METAL (2)			TRANSVERSE WELD (3)	
Test	Prod		0 2% Yield Strength ksi	Ultimate Strength ksi	Elongation in 2 in %	0 2% Yield Strength ksi	Ultimate Strength ksi	Elongation in 2 in %	Ultimate Strength ksi	
A1	A1	70	65 0	73 2	7.0	22 3	38 5	5 5	---	
B1	B1		65 0	73.2	8 3	22 2	39 8	7 0	---	
C4	C4		64.8	72.4	9 8	23 5	42.2	8 0	47 0	
C3	C3		64.1	72 8	10 3	23 4	42 7	8 0	48 4	
B2	B2		65.2	73 1	9 3	22.7	41 9	7 5	46.5	
D1	L2		63 1	72 3	10 5	23 5	42 2	---	45.5	
F2	L3	-320	71.9	85 6	10 0	34 8	47 3	3 5	43 0	
F3	H1		75.9	85 8	12 0	33 5	47 0	4 0	43 5	
G4	K3		72 1	84 1	14 5	29 2	45 7	4 0	41 7	
G2	G2		72 0	83 9	11 5	----	44 3	2 5	41 3	
G3	J1		75 4	84 7	12 0	33 5	46 5	4 0	39.2	
H1	F3		74 0	84 7	13 3	28.9	45 0	3 5	41.3	
H3	R3	-423	83 7	97 6	9 3	47 6	53 4	0 0	53 2	
H4	Q2		83 9	95 6	10 5	48 3	55 2	1 0	54.4	
I1	P2		84 7	96 5	8 8	42 4	49 7	0 0	46 1	

(1) Averages of 4 tests

(2) Averages of 2 tests

(3) Averages of 4 tests, all transverse weld coupons tested at 70°F

TABLE 11

AVERAGE UNIAXIAL TENSILE PROPERTIES OBTAINED FROM CONTROL COUPONS
TAKEN FROM CURED MIG-WELDED CYLINDER TRIM

Biaxial Specimen Code		Test Temp °F	UNIAXIAL PROPERTIES							
			PARENT METAL (1)			LONGITUDINAL ALL-WELD METAL (2)			TRANSVERSE WELD (3)	
Test	Prod		0.2% Yield Strength ksi	Ultimate Strength ksi	Elongation in 2 in %	0 2% Yield Strength ksi	Ultimate Strength ksi	Elongation in 2 in %	Ultimate Strength ksi	
B3	B3	70	65 9	71 9	9.3	36 6	46 7	3 0	29 1	
B4	B4		64 8	70 7	9 0	37 1	47 6	3.0	46 6	
C1	C1		66 5	72 3	8 8	36 6	47 1	3 5	55 7	
C2	C2	-320	65 6	85 6	9 0	36 4 (4)	48 8(4)	4 0(4)	50 5	
E2	N1		74 2	84 8	9 0	49 4	52 2	0 5	50 8	
H2	Q3		75 3	85 1	11 0	29 8	46 9	4 5	43 6	

(1) Averages of 4 tests

(2) Averages of 2 tests

(3) Averages of 4 tests, all transverse weld coupons tested at 70°F

(4) Tested at 70°F

TABLE 12

AVERAGE UNIAXIAL TENSILE PROPERTIES OBTAINED FROM CONTROL COUPONS TAKEN FROM UNCURED TIG-WELDED CYLINDER TRIM

Biaxial Specimen Code		Test Temp °F	UNIAXIAL PROPERTIES							
			PARENT METAL (1)			LONGITUDINAL ALL-WELD METAL (2)			TRANSVERSE WELD (3)	
Test	Prod		0 2% Yield Strength ksi	Ultimate Strength ksi	Elongation in 2 in %	0 2% Yield Strength ksi	Ultimate Strength ksi	Elongation in 2 in %	Ultimate Strength ksi	
J1	J3	70	61 4	71.8	10 0	23 5	46 0	10 5	49 6	
J2	E3		64 3	73 1	10 5	24.1	45 8	10 5	50 9	
J3	D1		64 6	72 9	9.0	25 0	45 8	9 5	49 3	
J4	H2		61 6	72 3	10 5	25 4	46 6	10 5	44.6	
K1	K1		60 6	71 3	11 0	29 7	46 0	11 5	46.8	
K2	K2		61 8	71 4	10.5	23 7	45 1	11 5	45.4	
L2	M1	-320	71 4	85 5	13 5	35 6	55 4	8.0	51 1	
K4S	M2		71 8	87 1	10 8	33 4	54 9	7 0	59 4 (4)	
L1S	H3		71 3	84 9	9 8	33 9	52 4	6 0	60.9 (4)	
K3S	M3		70 1	86.1	12 0	31 1	48 6	5 0	55.1 (4)	
L3	V3		72 7	85.8	11 8	31 8	52 4	6 5	50 3	
L4	S1		74 4	86 7	11 5	30 4	49 8	4 5	50 1	
I2	J2	-423	81 5	96 1	10 3	50 9	62 7	1 0	50 2	
I3	E1		79 7	91 4	9 8	51 6	62 6	1 0	49 8	
I4	T1		84 8	99 0	10 0	47 9	57 7	1 0	45 5	

(1) Averages of 4 tests

(2) Averages of 2 tests

(3) Averages of 4 tests, all transverse weld coupons tested at 70°F unless noted

(4) Tested at -320°F

TABLE 13

AVERAGE UNIAXIAL TENSILE PROPERTIES OBTAINED FROM CONTROL COUPONS
TAKEN FROM CURED TIG-WELDED CYLINDER TRIM

Biaxial Specimen Code		Test Temp °F	UNIAXIAL PROPERTIES							
			PARENT METAL (1)			LONGITUDINAL ALL-WELD METAL (2)			TRANSVERSE WELD (3)
Test	Prod		0 2% Yield Strength ksi	Ultimate Strength ksi	Elongation in 2 in %	0 2% Yield Strength ksi	Ultimate Strength ksi	Elongation in 2 in. %	Ultimate Strength ksi
D2	01	70	64 7	71 1	8 0	39 2	51.7	---	55 3
D3	02		64 6	70 8	7 8	39 0	51 5	6 0	55.7
D4	P1		64 5	71 1	8 0	40 3	51 1	5 0	52 1
E3	F2	-320	75 0	87 2	10 0	47 7	59 9	2 0	49 6
E4	K1		74 1	85 2	10 5	48 0	60 2	2 0	51 8
F1	Q1		73 7	83 9	10 8	46 6	59.2	2 0	52 0

(1) Averages of 4 tests

(2) Averages of 2 tests

(3) Averages of 4 tests, all transverse weld coupons tested at 70°F

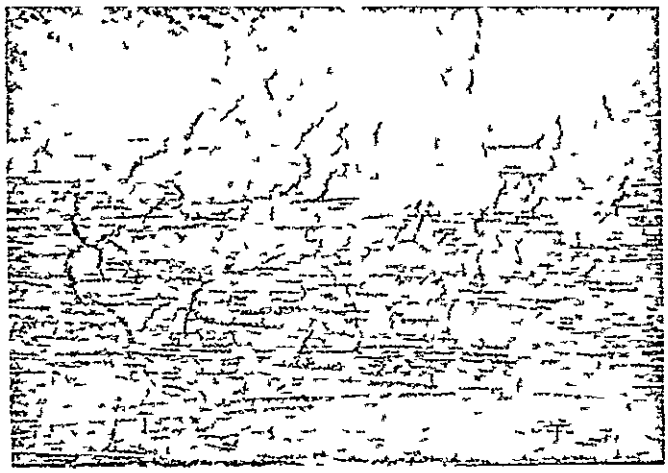

MAG 13X M20115

Figure 17 HAZ Cracking on O D Surface of Specimen B1 Observed after 2–to–1 (Axial–to–Hoop) Biaxial Test at 70° F

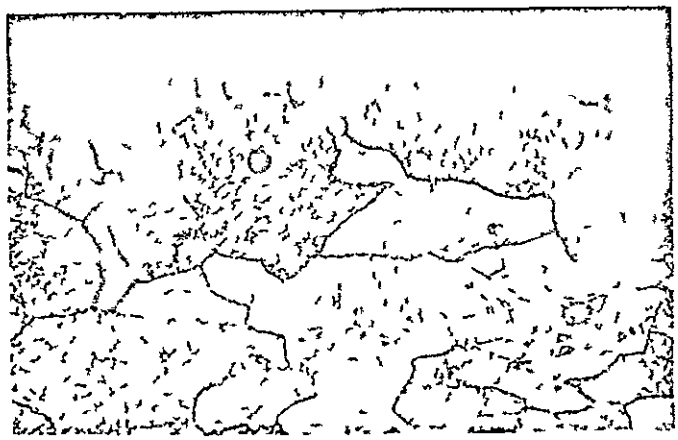

MAG 500X M20116

Figure 18 Cross-Section of HAZ Cracks Shown in Figure 17 Etchant Keller's Etch

c. In transverse weld coupons, ultimate strength at 70°F was increased 5 to 10% by curing.

Biaxial Strength Envelopes

Figures 19 through 23 are biaxial strength envelopes for MIG and TIG welded cylinders of 2014-T6 under the conditions tested in this program The biaxial envelopes were constructed as described above Theoretical biaxial envelopes are shown based upon Eq 2. The curves are solid when the experimental data agree reasonably well with the theoretical prediction The curves are dashed when the experimental data does not agree with the prediction or when sufficient experimental data do not exist to verify the prediction

In the biaxial strength envelopes truncated axial strengths occurred under certain test conditions indicating the possibility of longitudinal strain limitation in the welds At 70°F truncated axial strength was observed for cured MIG welds only The truncated axial strength for these welds was greater than the uniaxial parent metal tensile strength At -320°F, all welds, both cured and uncured, exhibited truncated axial strength generally greater than uniaxial parent metal tensile strength At -423°F, truncated axial strength was less than uniaxial parent metal tensile strength for both cured MIG and cured TIG welds

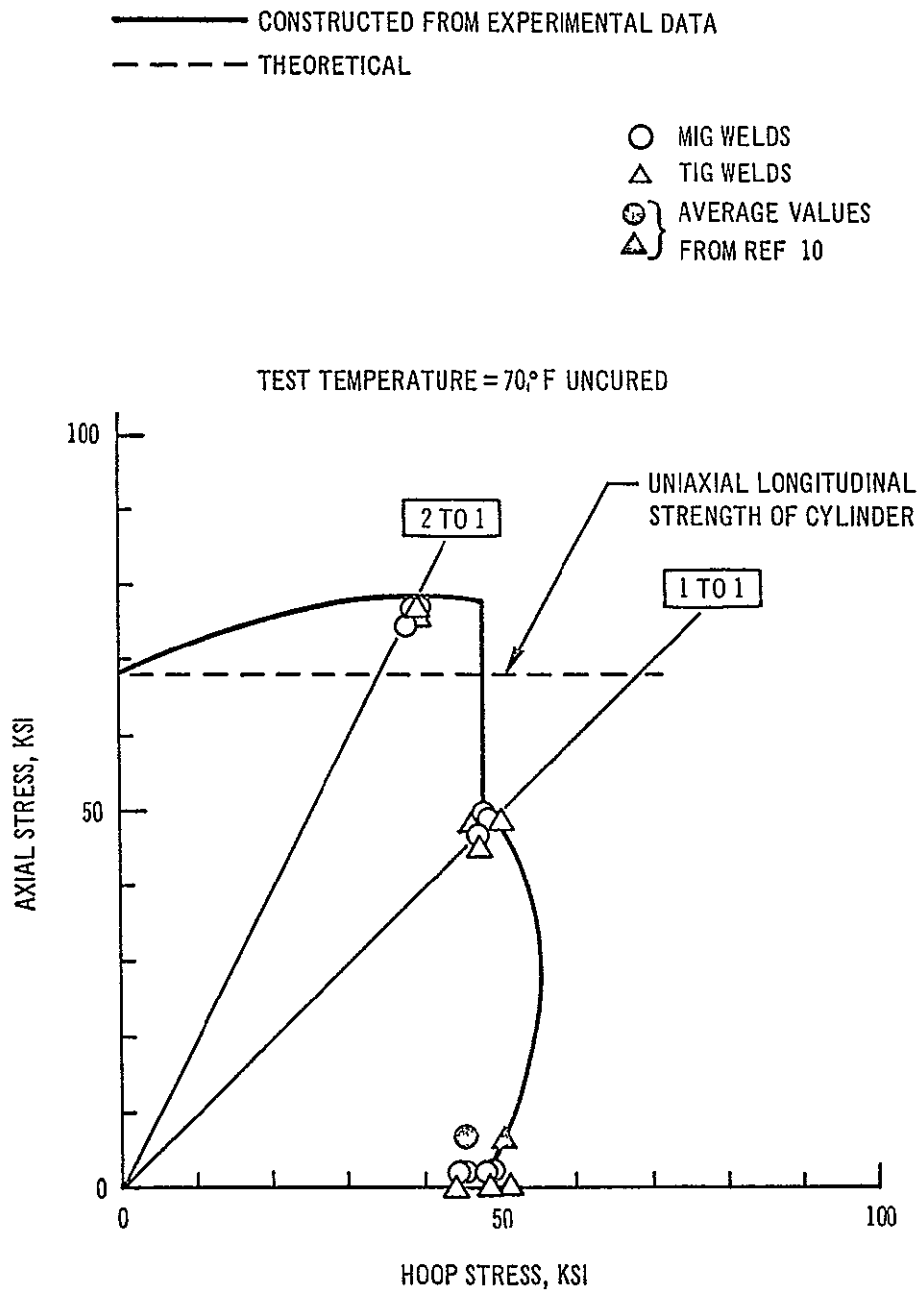

Figure 19 Biaxial Strength Envelope for As–Welded 2014–T6 Cylinders at 70° F

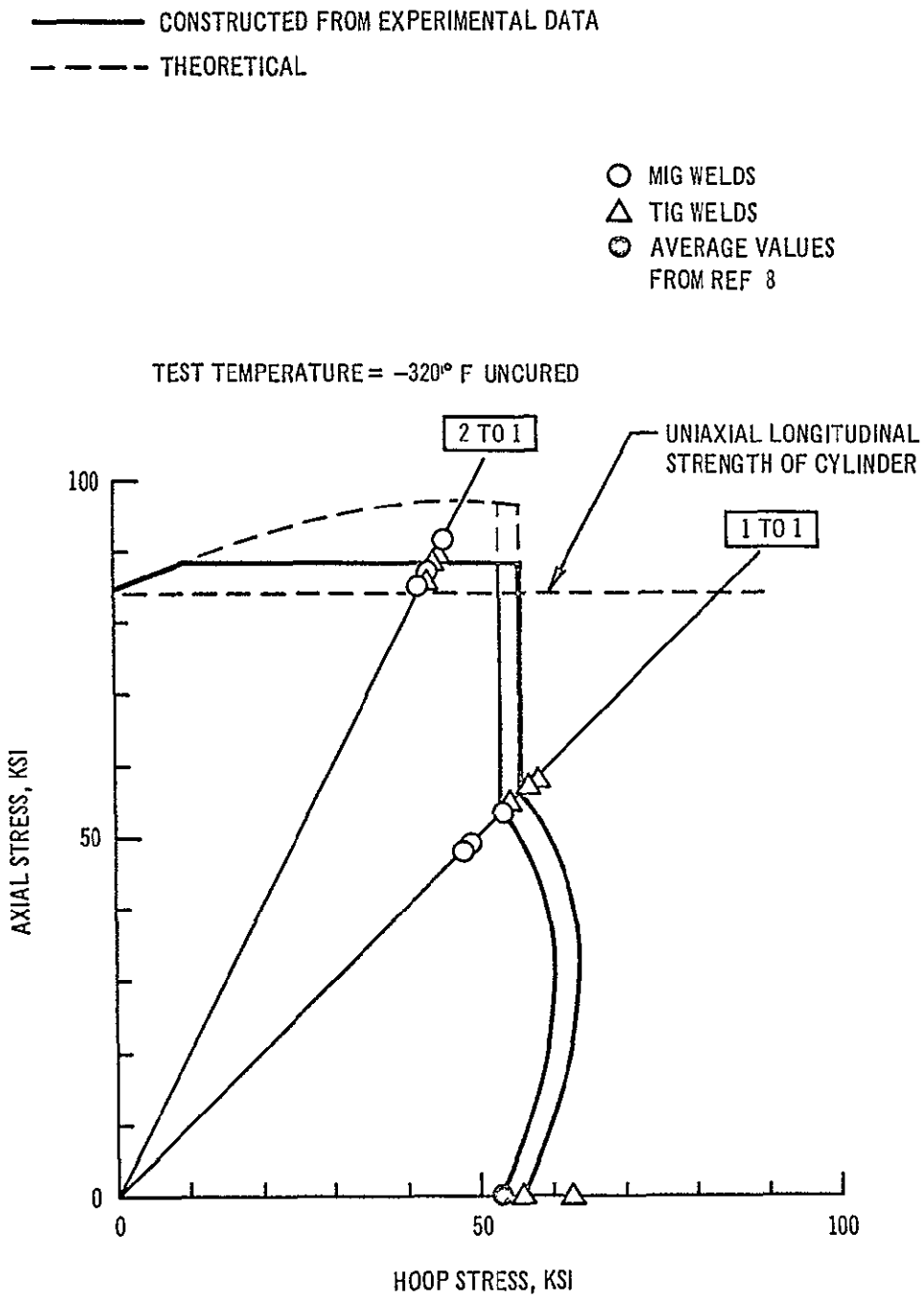

Figure 20 Biaxial Strength Envelope for As–Welded 2014–T6 Cylinders at –320°F

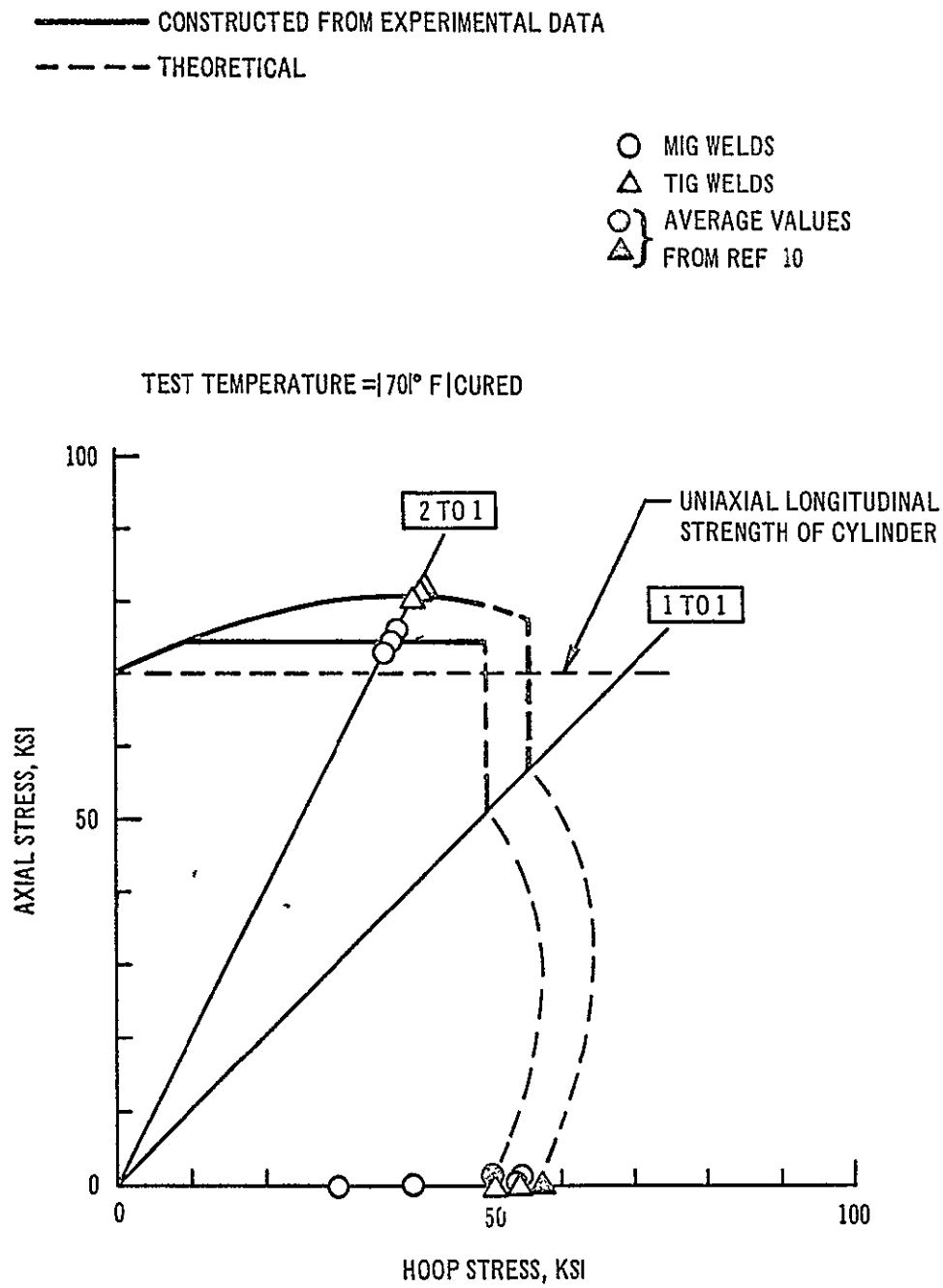

Figure 21 Biaxial Strength Envelope for Welded and Cured 2014–T6 Cylinders at 70° F

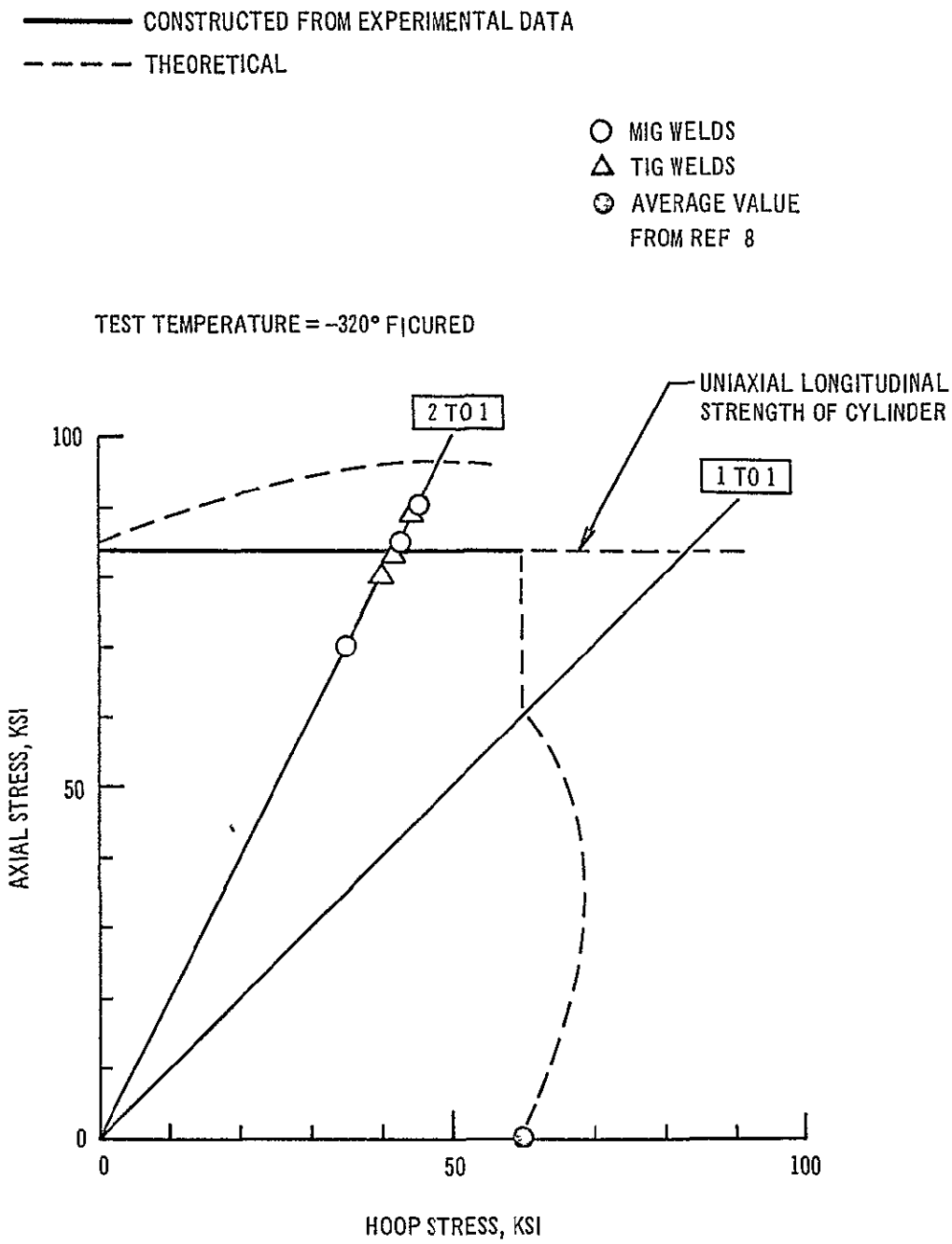

Figure 22 Biaxial Strength Envelope for Welded and Cured 2014–T6 Cylinders at –320° F

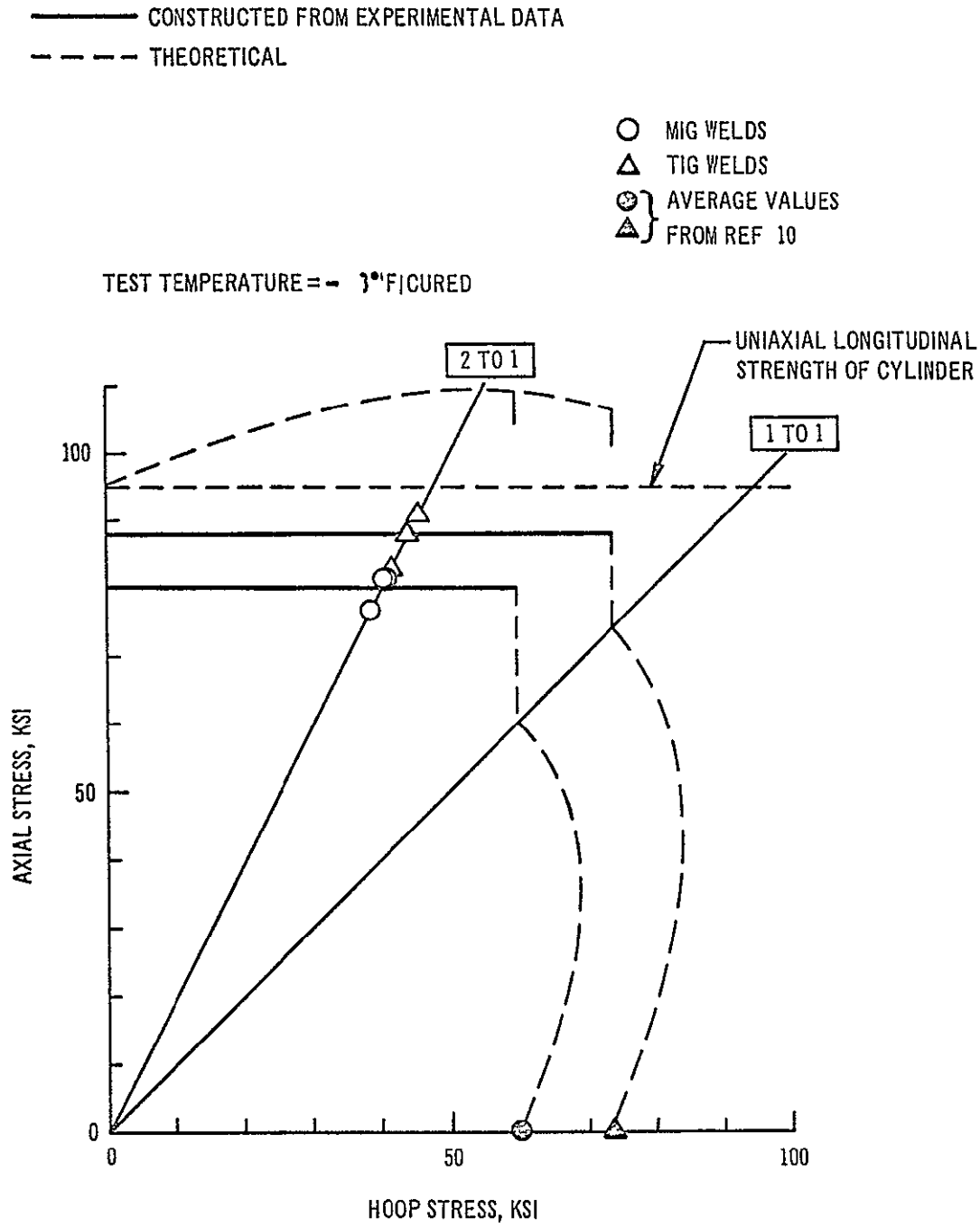

Figure 23 Biaxial Strength Envelope for Welded and Cured 2014–T6 Cylinders at –423° F

Transverse weld cracking at 70°F due to strain limitation in cured MIG welds has been observed in tests of specimens extracted from a scrapped common bulkhead aft (LOX) dome, as shown in Figure 24 Two specimens, 3-in wide in the reduced section and 16-in long, contained a portion of a meridion weld centered and parallel with the specimen loading axis (longitudinal) Each specimen was loaded in a tensile machine until a through crack initiated in the weld, at which time the specimen was unloaded The stress levels at which cracks were observed were 37 4 and 46 2 ksi in the two specimens As indicated in Table 4, the ultimate strength at 70°F of such panels is approximately 66 ksi

Since all cylinders subjected to 2-to-1 stress state tests at -423°F failed at stresses less than the parent metal biaxial 0 2% yield strength (1 15 X uniaxial 0 2% yield strength) Eq 7 can be applied to assess the correlation between failure stress of the cylinders and length of through crack at the time of burst Assuming that a through crack initiated in the weld due to longitudinal strain limitation and therefore extended from the fusion line on one side of the weld to the fusion line on the opposite side, then a value of K_c can be determined Rearranging Eq 7,

$$K_c = \left[\frac{\sigma_A^2 \, \pi \, \ell/2}{1 - \sigma_A^2/\sigma_y^2} \right]^{\frac{1}{2}} \qquad (8)$$

where σ_A = axial stress at failure of cylinder

σ_y = biaxial yield strength at -423°F = 94 3 ksi

ℓ = width of weld = length of through crack

2X M 18124

Figure 24 Transverse Crack Produced in Weld by Tensile Loading at 70° F of Coupon Cut from Common Bulkhead Insulation Adhesive Visible on Specimen Surface on Either Side of Weld

Measurements of weld width from metallographic cross-sections of MIG and TIG welds in 0 100 in thick sheet (Reference 10) suggested values for ℓ of 0.300 in and 0.220 in. for MIG and TIG welds, respectively. Table 14 presents the calculated K_c values for the -423°F biaxial tests. The values represent the critical plane stress stress-intensity for parent metal since failure of the cylinder is caused by propagation of the initial crack into and through parent metal, hence the average K_c values from the two sets of cylinders are equal regardless of weld process and variations in weld properties. These data indicate that where longitudinal weld strain limitation is a possibility, the weld process producing the narrowest weld is the more desirable

CONCLUSIONS

1. In a biaxial stress state of 1-to-1 (axial-to-hoop), the limiting strength of welded 2014-T6 is the transverse weld strength

2 In a biaxial stress state of 2-to-1 (axial-to-hoop), the limiting strength of welded 2014-T6 is the axial composite strength elevated 10 to 15% above uniaxial (1-to-0) strength unless longitudinal weld ultimate strain limits the axial strength

   a For uncured MIG and TIG welds in 2014-T6, longitudinal weld ultimate strain does not limit axial strength at 70°F, but reduces axial strength at -320°F to about 105% of uniaxial strength

TABLE 14

VALUES OF K_c CALCULATED FOR 2-TO-1 BIAXIAL TESTS AT -423°F

Biaxial Specimen Code		Weld Process	Width of Weld ℓ in	Axial Stress σ_A ksi	K_c (Eq 8) ksi$\sqrt{\text{in}}$	Average K_c ksi$\sqrt{\text{in}}$
Test	Prod					
H3	R3	MIG	300	81 5	70 6	
H4	Q2			81 6	70 8	68 7
I1	P2			77 0	64 7	
I2	J2	TIG	220	83 7	63 2	
I3	E1			88 2	68 2	68 4
I4	T1			91 2	73 7	

b For cured MIG welds in 2014-T6, longitudinal weld ultimate strain limits axial strength to about 105% of uniaxial strength at 70°F, 100% of uniaxial strength at -320°F, and 85% of uniaxial strength at -423°F

c For cured TIG welds in 2014-T6, longitudinal weld ultimate strain does not limit axial strength at 70°F, but reduces axial strength to 100% of uniaxial strength at -320°F and to 93% of uniaxial strength at -423°F

3 When longitudinal weld strain limitation occurs in welded 2014-T6, it results in reduced biaxial strength probably caused by the formation of through cracks across the weld

4. Longitudinal weld strain limitation effects are less in TIG-welded 2014-T6 than in MIG-welded 2014-T6 probably because of the narrower weld produced by TIG welding

5. On the basis of 70°F and -320°F tests of uniaxial coupons taken from the cylinder trim, the curing cycle has the following effects

a Curing has essentially no effect on parent metal properties determined at 70° and -320°F

b From longitudinal all-weld metal tests curing produces increases of approximately 50% and 10% in yield and ultimate strengths, respectively, regardless of weld process, at 70° and -320°F. These increases are accompanied by a reduction of about 50% in elongation

c. From transverse weld tests at 70°F, curing increases ultimate strength approximately 5 - 10%, regardless of weld process.

6. On the basis of tests of uniaxial coupons taken from the cylinder trim, TIG welds exhibit higher yield strength, ultimate strength and elongation than MIG welds compared at the same test temperature, in the same cure state and in the same specimen orientation

REFERENCES

1. "Strength Tests of MIG and TIG Welds in 2 1 and 1:1 Biaxial Stress Fields at Normal Atmospheric Temperature and at LN_2 and LH_2 Temperatures", Technical Memorandum No 105, Douglas Aircraft Company, 13 February 1967.

2 Theory of Flow and Fracture of Solids, Nadai, McGraw-Hill, 1950

3 Theory of Plasticity, O Hoffman and G Sachs, McGraw-Hill, 1953

4. "UCLA Engineering 163A Syllabus", G H Sines, University of California at Los Angeles

5 "Plastic Instability of Pressure Vessels", N M. Harrington, Report SM-38785, Douglas Aircraft Company, 29 August 1960

6 "The Biaxial Properties of Titanium Alloys at Cryogenic Temperatures", S F. Frederick and D. L Corn, Douglas Paper No. 4257, Douglas Aircraft Company, Santa Monica, California, 18 April 1967

7. "A Theory of Yielding and Plastic Flow of Anisotropic Metals", R Hill, Proceedings of the Royal Society, Vol 193, Serial A, 1948, p 281

8. "MIG Uniaxial Weld Design Allowables Test Program", R W McIver, Report MP 20,450, Douglas Aircraft Company, 24 May 1965.

9. "Fracture Testing of High Strength Sheet Materials", Anon , ASTM Bulletin, No 243, January 1960

10 "Evaluation of MIG and TIG Welding Processes for Joining 2014-T6 Aluminum Alloy - Phase I", R J. Davis, R N Hooker, E F Kaluza, Report SM-48383, Douglas Aircraft Company, 21 January 1965

MISSILE & SPACE SYSTEMS DIVISION/SPACE SYSTEMS CENTER
5301 BOLSA AVENUE, HUNTINGTON BEACH, CALIFORNIA
A DIVISION OF DOUGLAS AIRCRAFT COMPANY, INC.